Shootin1a mediates an F-actin-adhesion clutch for dendritic spine formation and synaptic plasticity

Ria Fajarwati Kastian
Nara Institute of Science and Technology
Division of Biological Sciences
Laboratory of Systems Neurobiology and Medicine
Supervisor: Professor Naoyuki Inagaki

Submitted on 2019/09/17

Graduate School of Biological Sciences Doctoral Thesis Abstract

Lab name (Supervisor)	Systems Neurobiology and Medicine (Naoyuki Inagaki)		
Name (Surname)(Given name)	Ria Fajarwati Kastian	Submission Date	2019/07/29
Title	Shootin1a Mediates an F-actin-adhesion Clutch for Dendritic Spine Formation and Synaptic Plasticity		

Dendritic spines are tiny protrusions emerging from dendritic shafts of excitatory neurons and form synaptic contacts with the presynaptic terminals of axons. These structures have been thought to represent the main unitary postsynaptic compartment for excitatory input. Dendritic spines contain a highly organized structure, postsynaptic density (PSD), which is characterized by a high density of receptors and channels, associated signaling molecules and adhesion molecules.

The morphology of spines has been classified based on their appearance as filopodia-like, thin, stubby and mushroom-shaped types. Filopodia-like spines are more prominent in the developing brain at early postnatal stages and diminish with adulthood. Hence, filopodia-like spines are thought to be the precursor of dendritic spine. Synaptic contacts become established when filopodia-like spines select the target axons and form synaptic connections. Notably, in response to the synaptic activation, dendritic spines undergo structural changes that rely on actin polymerization. In addition, long-term potentiation (LTP), an activity-dependent plasticity at synapse, is thought to underlie the learning and memory. Extensive studies have shown that actin cytoskeleton and its regulatory proteins play important roles in the dendritic spine formation, maturation and synaptic plasticity. However, the molecular mechanics how actin reorganization leads to the structural alteration of spines remains unknown.

The alterations of the spine number and morphology are observed in many types of brain disorders. Intellectual disability, autism spectrum disorder (ASD), schizophrenia and Alzheimer`s disease are neurological disorders that are reported to have alteration in size, shape and density of dendritic spines. Early-onset developmental disorder, such as intellectual disability and ASD are associated with too few or too many of dendritic spine number, respectively. Moreover, post mortem studies reported that a high number of filopodia-like and thin spines in the brains of intellectual disability individuals, indicative of immature spines. Schizophrenia is brain disorder affecting thought, perception of reality, affect and cognition, which typically found in the early adulthood or late adolescence. A study has been found that spine density in the schizophrenia is decreased. Lastly, decreased in dendritic spines in the hippocampus and cortex is also found in Alzheimer`s disease. Based on these observations, it is believed that dendritic spines serve as a common substrate for neuropsychiatric disorders, particularly for those involve deficit in processing information.

Shootin1a, a brain specific protein, has been known as a clutch molecule. During early developmental stages of neurons, shootin1a mediates the force transmission from actin cytoskeleton to the substrate in order to induce axon formation and guidance. In this study, I found the accumulation of shootin1a in dendritic spines. Here, I hypothesized that shootin1a may play a role in the formation and plasticity of dendritic spines.

First, to investigate whether shootin1a is localized in dendritic spines, hippocampal neurons

were isolated from E18 rat and cultured on dishes or glass coverslips. Immunoblot analyses showed that shootin1a is detected not only on the early stages, Day In Vitro (DIV) 3, but also in the later stages (DIV 7, DIV 14 and DIV 28) of cultured hippocampal neurons. By contrast, shootin1b, a splicing variant of shootin1a, was not detected in the later stages (DIV 14 and DIV 28). Immunocytochemistry analyses showed that shootin1a is accumulated at the tip of filopodia-like spines and co-localized with stubby spines. Moreover, shootin1a was also found to co-localize with PSD-95, a postsynaptic marker. The localization of shootin1a in dendritic spines raises the possibility that shootin1a may be involved in the dendritic spine formation. To further examine whether shootin1a is required for dendritic spine formation, I performed shootin1 knock down analysis. I found that suppression of shootin1 with shootin1-RNAi decreased the number of PSD-95 in a low-density culture of rat hippocampal neurons. Similar data were also obtained with hippocampal neurons cultured from shootin1-KO mice. *In vivo* data also showed that shootin1-KO mice brain exhibited a low number of dendritic spines and interestingly, mature spines was significantly decreased in shootin1a-KO mice. In contrast, overexpression of shootin1a led to an increased number of PSD-95-positive puncta. Together, these data indicate that shootin1a mediates the formation and maturation of dendritic spines.

Second, I examined whether shootin1a functions as a clutch molecule in dendritic spines. Shootin1a was reported to interact with actin binding protein, cortactin, and cell adhesion molecule, L1-CAM. These interactions transmit the force of F-actin retrograde flow to the adhesive substrate, thereby generating force for axon outgrowth. Moreover, our previous study reported that clutch coupling between F-actin and substrate reduces the speed of F-actin flow in axonal growth cone. Immunocytochemical analysis revealed that shootin1a is co-localized with cortactin, F-actin, and L1-CAM. Additionally, overexpression of shootin1a (1-125), a dominant negative mutant to disrupt the shootin1a-L1-CAM interaction, increased the velocity of F-actin in the filopodia-like spines. These data suggest that shootin1a functions as a clutch molecule in dendritic spines and that shootin1a (1-125) inhibits shootin1a-mediated clutch coupling. Using traction force microscopy, I further examined whether spines generate force. Traction forces under the spines were monitored by visualizing force-induced deformation of the elastic substrate, which is reflected by displacement of the beads from their original positions. As the results, the beads moved dynamically under the filopodia-like spines, indicating that force is generated at spines. Interestingly, inhibition of shootin1a-mediated clutch coupling by overexpression of myc-shootin1a (1-125) significantly reduced traction force generation in spines, which in turn resulted in a decreased number of dendritic spines. Together, these findings demonstrate that shootin1a functions as a clutch molecule and mediates the generation of force for dendritic spine formation.

Finally, I investigated whether shootin1a is involved in the synaptic plasticity. Hippocampal neurons were stimulated with glutamate, a major neurotransmitter in brain. Immunoblot analysis showed that glutamate stimulation induced PAK1-mediated shootin1a phosphorylation. In addition, the results obtained from the chemical LTP technique showed that spine enlargement induced by NMDA receptor activation was inhibited by overexpression of shootin1a (1-125). These data suggest that shootin1a plays an essential role in activity-dependent spine enlargement during LTP.

In conclusion, this study demonstrates that shootin1a, as a clutch molecule, mediates mechanical regulation for dendritic spine formation, maturation and spine plasticity. This work also provides intriguing insights about the molecular mechanics of dendritic spines alterations in neuropsychiatric disorders.

Table of Contents

1. Introduction

1.1 Dendritic spine is a key element for learning and memory and substrate for neuropsychiatric disorders

It is nearly impossible to begin my doctoral thesis without citing a Spanish neuroscientist and anatomist, Sandiago Ramón y Cajal (1852-1934). His incredible anatomical skills and tireless working habit has contributed to the first theories about synapses, synaptic transmission and synaptic plasticity (Mateos-Aparicio and Rodríguez- Moreno, 2019). Cajal first described the dendritic spines as points of contacts with excitatory axon terminals. The predominant idea postulated by Cajal is that nerve impulses flow from the terminals of the presynaptic neuron to the dendritic tree and out through the axons of the postsynaptic neurons (Llinás, 2003; Sotelo, 2003). Cajal also proposed that the capacity of the brain could be augmented by increasing the number of connections (DeFelipe, 2006). Generation of neuroscientists have extended these early concepts, showing that dendritic spines on pyramidal neurons are highly plastic and appear to be a key element for learning and memory (Hammond et al., 2015; Borczyk et al., 2019).

Learning and memory are thought to be basic functions of the brain. The mechanisms underlying these brain functions are assumed to involve synaptic plasticity (Frankfurt and Luine, 2015). Learning elicits activity in a neural network that results in modification of the strength of synaptic connections. Information is stored in the form of these synaptic alterations, and the pattern of alterations is thought to constitute the memory trace. Synaptic plasticity is thought to mediate the acquisition, consolidation and retention of the memory (Bear and Malenka, 1991; Malenka and Bear, 2004).

Neuronal dendrites of excitatory neurons are decorated by dendritic spines, where the excitatory synapses are terminated. Subtle changes in the number, size and shape of the spines may have marked effects on synaptic function and plasticity. Notably, neuropathological studies reported that number of spines is decreased in Alzheimer`s disease, intellectual disability and schizoprenia, whereas autism spectrum disorders (ASD) seemed to be characterized by an increased spine number (Penzes et al., 2011) (Figure 1). The brain of intelectual disability individuals exhibited a high number of immature spines, filopodia-like and thin spines (Moyer et al., 2015; Forrest et al., 2018). In addition, it was reported that brain section of fragile X syndrome patient has abnormally immature and unstable spines, which may lead to defect in synaptic contacts (Cruz-Martín et al., 2012). Dendritic spine alteration

in neurological disorders can be caused by abnormality of presynaptic input, changes in neuron-autonomous functions, or extraneuronal factors (Herms and Dorostkar, 2016). Thus, dendritic spines are thought to serve as a substrate for neuropsychiatric disorders, particularly those involving deficit in processing information.

1.2 Morphogenesis of dendritic spines

The morphology of dendritic spine is classified into filopodia-like, thin, stubby, mushroom- and cup-shaped (Hering and Sheng, 2003) (Figure 2A). During development, neurons are first decorated by filopodia-like spine, extending 5 – 10 μm in length. *In vitro* studies reported that day in vitro (DIV) 7 - 11 cultured hippocampal neurons are abundant in filopodia-like spines. As development proceeds, filopodia-like spines are then subsequently decreased and replaced with mature spines, i.e. thin and mushroom-shaped. Mature spines are mostly found in DIV 14 - 28 cultured neurons (Korobova and Svitkina, 2010).

Filopodia-like spine are highly dynamic and motile, and are believed to serve as early synapse (Portera-Cailliau et al., 2003; Nimchinsky et al., 2002). The high motility of filopodia-like spines may increase their probability chance encounter between axons. Mature spines consist of three distinct compartments: (1) a base at the junction to the dendritic shaft, (2) a constricted neck in the middle, and (3) a bulbous head contacting the axon (Figure 2B). They have a wide range of sizes and shapes, 0.2 – 2 μm in length and volume is 0.001 – 3 μm^3. Thin spines are most common and have a long neck with a small bulbous head. Mushroom-shaped spines are those with a large head and shorter neck. Stubby spines are devoid of neck (Ziv and Smith, 1996; Hering and Sheng, 2001; Hotulainen and Hoogenraad, 2010). In addition, a recent analysis using super resolution microscope reported that ~70% of spines that appeared globular or cup-shaped exhibit more complex structures with several finger-like extension (Chazeau et al., 2014).

The volume of dendritic spine head was shown to correlate with the size of postsynaptic density (PSD), an electron-dense region attached to the postsynaptic membrane. PSD connects with actin cytoskeleton (Sheng and Hoogenraad, 2007; Bosch et al., 2014) and provides a structural framework for localizing functional molecules including neurotransmitter receptors and ion channels. The strengthening or weakening of synaptic activity is reported to associate with the volume of spine head and the size of PSD area (Hering and Sheng, 2001; Borczyk et al., 2019).

Actin cytoskeleton and its regulatory proteins are the major spine components involved in dendritic spine formation, maturation and modification (Tada and Sheng, 2006;

Hotulainen and Hoogenraad, 2010; Tatavarty et al., 2012; Basu and Lamprecht, 2018). Dendritic morphogenesis is proposed to begin from actin patch elongating into dendritic filopodium, where the tip subsequently expands via actin nucleating factors, formin mDia2 and Arp2/3 proteins. The length of spines is modulated by myosin II-dependent contractility (Korobova and Svitkina, 2010). In addition, actin capping protein (CP) and cortactin are also reported to play a key role during remodeling of actin architecture underlying spine morphogenesis (Hering and Sheng, 2003; Fan et al., 2011; Korobova and Svitkina, 2010; Lei et al., 2016; Koganezawa et al., 2016). Interestingly, a study demonstrated that Arp2/3-mediated branched nucleation occurs in specific nano-domains at PSD and formin-dependent actin polymerization drives the formation of finger-like protrusion from the side of the spine head (Chazeau et al., 2014).

1.3 Activity-regulated dendritic spine plasticity

The morphological changes in dendritic spines occur during long-term potentiation (LTP) and long-term depression (LTD). LTP is accompanied with the formation of spine and the enlargement of spine head, whereas LTD is accompanied with the shrinking and retraction of spines (Tada and Sheng, 2006). *In vivo* studies have revealed that both tetrodoxin (TTX) and glutamate application on brain slices could increase the number and the length of dendritic filopodia (Portera-Cailliau et al., 2003). In addition, study *in vitro* has reported that activated spines by the release of caged glutamate showed an increase in F-actin pool within the spine head (Matsuzaki et al., 2001; Fukazawa et al., 2003; Honkura et al., 2008). Polymerization and de-polymerization of F-actin are the critical process for the induction and maintenance of long-term potentiation. The increment of F-actin polymerization after LTP stimulation is dependent on NMDA receptor activation and inactivation of actin depolymerizing factor/cofilin (Fukazawa et al., 2003).

Glutamate binds to postsynaptic glutamate receptor channels, AMPA (α-amino-3-hydroxy-5-methyl-4-isoxazolepropionic acid) receptor and NMDA (N-methyl-D-aspartic acid) receptor, which open to allow ion Na^+ and Ca^{2+} influx, respectively, thereby triggering a series of signaling pathways. A predominant pathways for LTP is dependent on NMDA receptor activation and subsequent calcium influx (Tanaka et al., 2008; Fortin et al., 2010). Calcium influx promotes the activation of a serine/threonine protein kinase, Ca^{2+}/Calmodulin-dependent protein kinase II (CaMKII), which in turn mediates spine expansion via a rapid polymerization of F-actin and induces the translocation of specific proteins to the synapse (Okamoto et al., 2007; Redondo and Morris, 2011; Bosch et al., 2014). The Rho family of

small GTPases, RhoA and Rac1/Cdc42, are also known to contribute to the dendritic spine growth and stability (Newey et al., 2005; Murakoshi et al., 2011). Furthermore, the main downstream effector of Rac1/cdc42, Pak1 (p21-activated kinase 1) kinase, regulates spine formation and synaptic plasticity (Hayashi et al., 2004, 2007; Asrar et al., 2009)

1.4 Shootin1a

Shootin1a is a brain specific protein that was identified in our laboratory (Toriyama et al., 2006; Higashiguchi et al., 2016). Our laboratory also reported a shootin1a splicing variant, shootin1b, which is expressed not only in the brain but also in the peripheral tissues (Higashiguchi et al., 2016; Minegishi et al., 2018). Shootin1a has 456 amino acid residues, whereas shootin1b has 631 amino acid residues (Figure 3). Both shootin1a and shootin1b consist of three coil-coiled regions and a single proline-rich region. The residues 261-377 directly interacts with actin-binding protein, cortactin, while the residues 1-125 is essential for directly binding to cell adhesion molecule, L1-CAM (Kubo et al., 2015; Baba et al., 2018).

Shootin1a is involved in axon outgrowth and guidance (Toriyama et al., 2006; Shimada et al., 2008; Kubo et al., 2015; Baba et al., 2018). Interaction of shootin1a and cortactin in axonal growth cone couples F-actin retrograde flow with extracellular adhesive substrates via L1-CAM to transmit force of F-actin retrograde flow to the substrate (Toriyama et al., 2013; Kubo et al., 2015; Baba et al., 2018) Additionally, netrin-1 induces Pak-1 mediated shootin1a phosphorylation via activation Cdc42 and Rac1. The phosphorylation of shootin1a enhances shootin1a interaction with cortactin and L1-CAM, thereby producing traction force for axon guidance (Toriyama et al., 2013; Kubo et al., 2015; Baba et al., 2018) (Figure 4). However, the functions of both shootin1a and shootin1b in mature neurons are unknown.

1.5 Research objectives and findings

The objective of this doctoral thesis is to investigate the role of shootin1 in the later stages of developmental hippocampal neurons. I found that shootin1a is localized in dendritic spines. Thus, I continued this study by examine the roles of shootin1a in dendritic spines. Moreover, the underlying mechanism of the formation, maturation, and synaptic plasticity mediated by shootin1a is also studied. Here, I propose that shootin1a mediates F-actin adhesion coupling for the spine formation, maturation, and plasticity. I demonstrated that the generation of traction force in dendritic spines from F-actin retrograde flow to substrate is mediated by shootin1a. Finally, this study showed that shootin1a is involved in NMDA receptor-spine enlargement, which may underlie learning and memory.

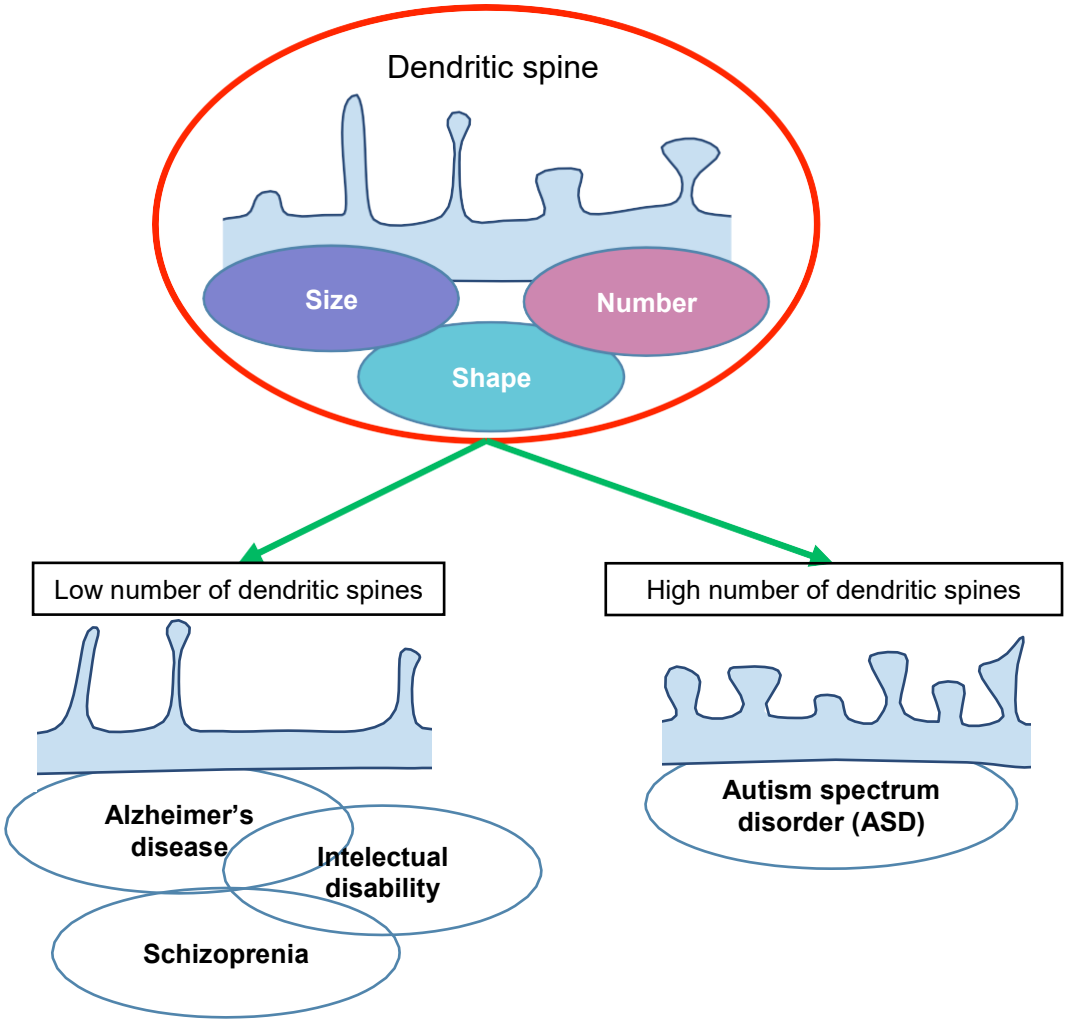

Figure 1. Dendritic spine pathology in neuropsychiatric disorders, such as Alzheimer`s disease, Intelectual disability, Schizoprenia, and ASD

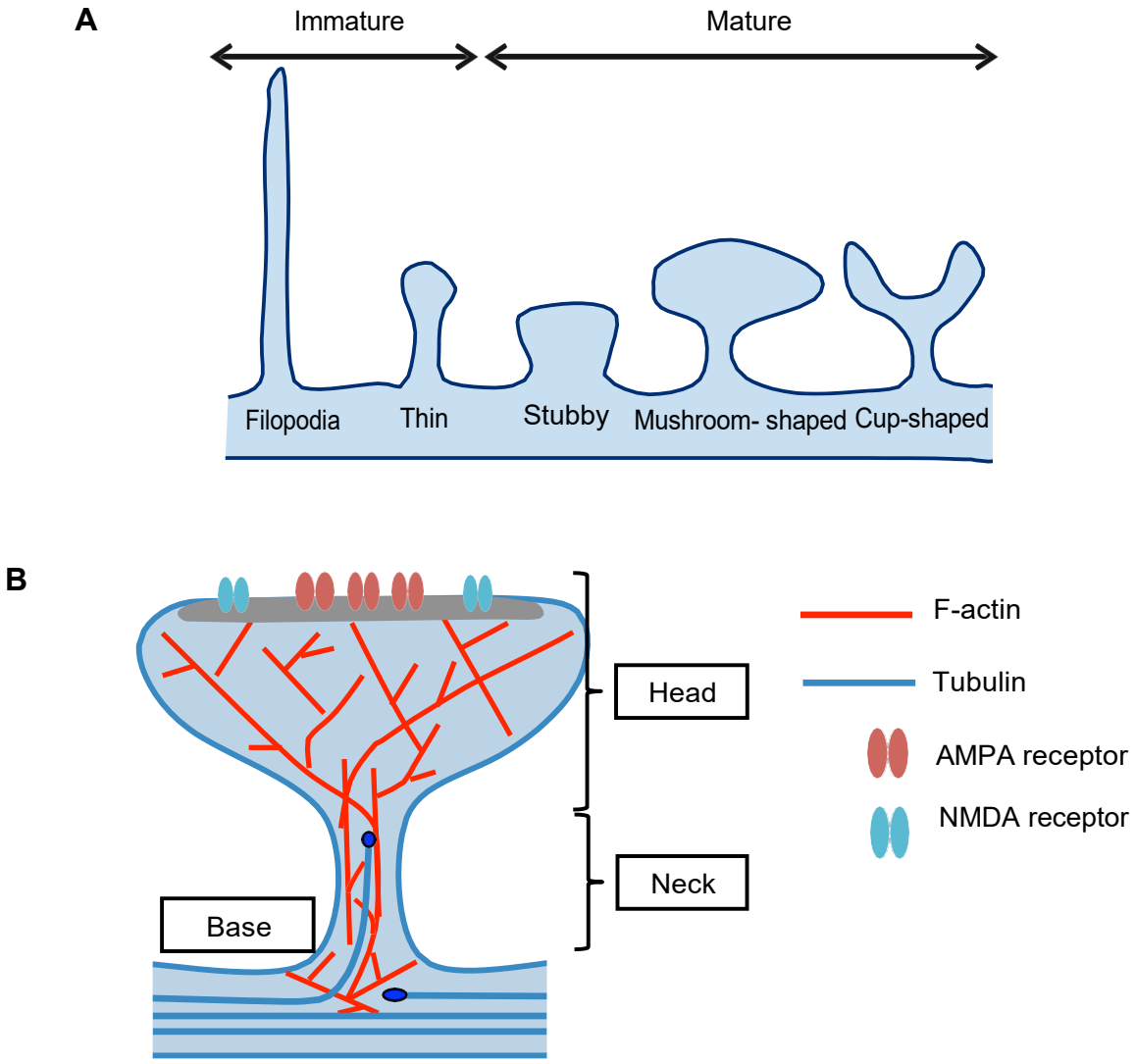

Figure 2. (A) Morphological classification of dendritic spines. Filopodia-like and thin spines are immature spines, whereas stubby, mushroom- and cup-shaped spines are mature ones. (B) Mature spines consist of three distinct basic compartments: Head, neck, and base.

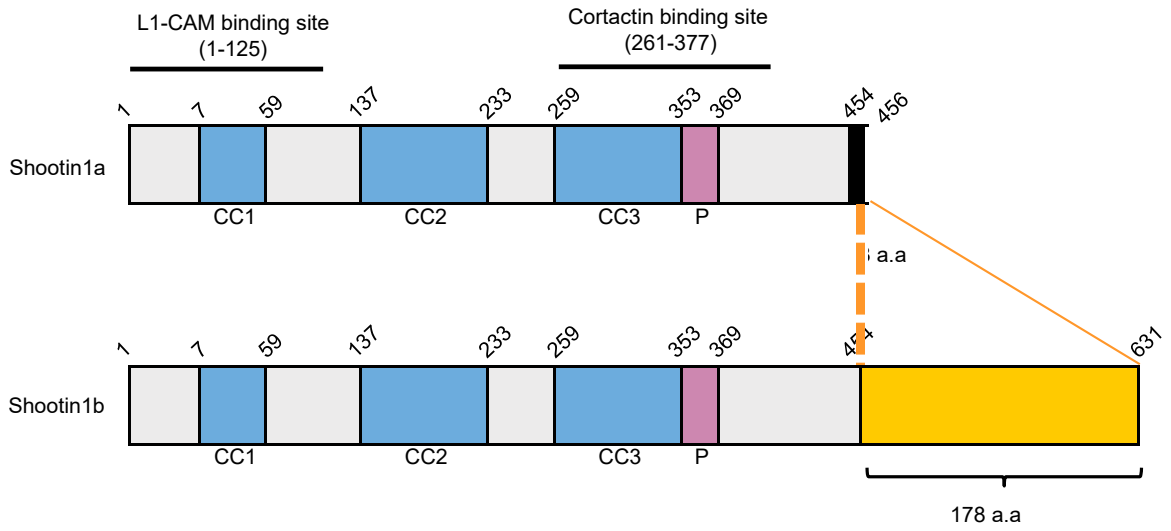

Figure 3. Splicing variants of shootin1. Shootin1 contains three coil-coiled regions (CC) and a single proline-rich (P) region. Shootin1a and shootin1b have 3 and 178 amino acids specific at their C-terminal regions, respectively.

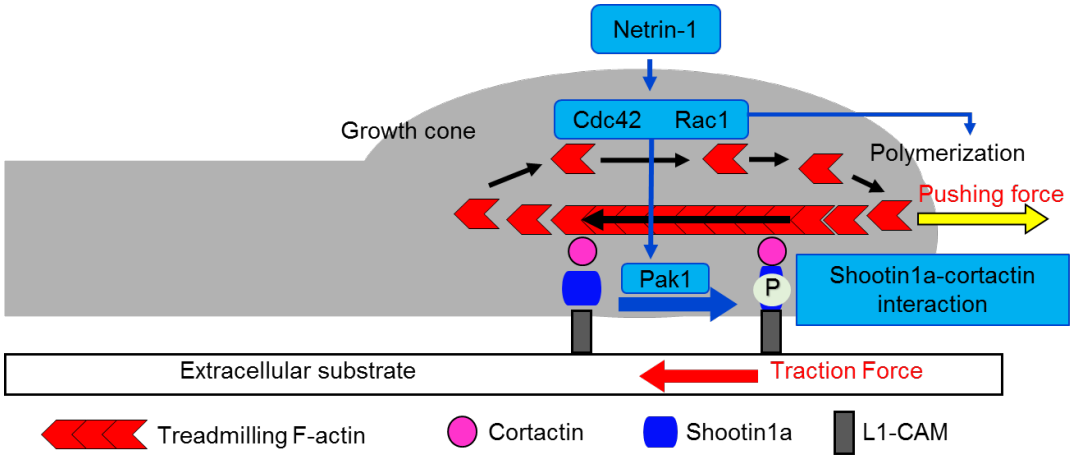

Figure 4. Shootin1a functions as a clutch molecule to generate traction force for axon outgrowth. Pak1-mediated shootin1a phosphorylation by netrin-1 signaling transmits the force of F-actin retrograde flow (black arrow) onto the extracellular substrate (red arrow).

2. Materials and Methods

2.1 Materials

2.1.1 Antibodies

Rabbit polyclonal anti-shootin1a and anti-shootin1b peptide antibodies were prepared as described (Higashiguchi et al., 2016; Baba et al., 2018). The rabbit polyclonal anti-shootin1, anti-pSer101-shootin1, and anti-pSer-249-shootin1 antibodies were prepared as previously described (Toriyama et al., 2006, 2013). Mouse anti-PSD-95 was obtained from Thermo Scientific (Cat# MA1-045). Mouse anti-actin (Cat# MAB 1501-R) and mouse anti-cortactin (Cat# 05-180) were obtained from EMD Millipore. Mouse anti-synaptophysin (Cat# Sc-5507) and goat anti-NCAM-L1 (Cat# Sc-1508) were purchased from Santa Cruz Biotechnology. Rabbit anti-myc (Cat# 562-5) and rabbit anti-GFP (Cat# 598) were purchased from MBL. The following secondary antibodies were used: rabbit anti-IgG secondary antibody Alexa Fluor 594 (from donkey) (Cat# 711-585-152) was obtained from Jackson Immuno Research Labs, whereas anti-goat Alexa Fluor 488 (from donkey) (Cat# A-11055) and anti-mouse IgG Alexa Fluor 488 (from donkey) (Cat# A-11029) were obtained from Thermo Fisher Scientific. HRP-conjugated donkey anti-rabbit IgG (Cat# NA934), HRP-conjugated goat anti-mouse IgG (Cat# AP308P) and HRP-conjugated donkey anti-goat IgG (Cat# AP180P) were obtained from GE Healthcare, Thermo Fischer Scientific and Millipore, respectively.

2.1.2 Plasmids

The shootin1a expression plasmid was prepared as described previously (Toriyama et al., 2006). Recombinant DNA reagent pFN21A-HaloTag-actin, pFN21A-HaloTag-cortactin and pFN21A-Halotag-shootin1a were previously described (Katsuno et al., 2015; Kubo et al., 2015). To generate cDNA fragments of dominant negative of shootin1a, shootin1a deletion mutants were amplified by PCR and subcloned into pGEX-6P-1 (GE Healthcare, Cat# 28954648), pCAGGS-myc, pCAGGS-EGFP, pCMV-myc (Stratagene) or pEGFP (Clontech) vectors (Baba et al., 2018). The generation of pCAGGS-myc-shootin1a was used to overexpress shootin1a protein under β-actin promoter as described previously (Toriyama et al., 2006). The cDNAs of human β-actin was cloned into pAcGFP-C1 (Clontech Laboratories).

2.1.3 Animals

Rats and C57BL/6 mice were obtained from SLC Japan and CLEA Japan, repectively. *Shootin1* knockout mice were generated by replacing the first exon of *Shootin1* with IRES-*LacZ* and PGK-neo. The linearized targeting vector was introduced into donor ES cells and then ES cells with positive clone were injected into C57BL/6 mice blastocyst to generate chimeric mice. Chimeric mice were crossed with C57BL/6 mice for at least seven generations before analysis to ensure the genetic background (Baba et al., 2018).

2.2 Culture of hippocampal neurons

Embryos were removed from the uterus and placed on ice. The whole brains were carefully removed by excision of the soft skull, and the whole brains were submerged in 0.4% glucose/PBS solution for dissection of the hippocampus. Briefly, the isolated hippocampus was conducted under the dissecting microscopy. After removing the meninges layer of the cerebrum, the hippocampus was carefully removed using sharp autoclaved forceps. Hippocampi were transferred into sterile filtered Solution A^+ (0.5mg mL^{-1} papain; 6 µg mL^{-1} DNase I; 1 mg mL^{-1} BSA; 0.01 M glucose; MilliQ water) and incubated in 37°C water bath for 20 minutes. Solution A^+ was the removed and replaced with 10 mL Solution A^- (6 µg mL^{-1} DNase I; 1 mg mL^{-1} BSA; 0.01 M glucose; MilliQ water). Hippocampi were triturated by gently pipetting the solution up and down and then incubated dissociated hippocampi in 37°C water bath for 15 minutes. Genetic materials were removed from the cell suspension by swirling a glass Pasteur pipette. Cell suspension was collected by centrifugation (4°C, 1500 RPM, 20 minutes) and Solution A^- was removed and re-suspended in PBS solution. Cell was then counted using hemocytometer with tryphan blue staining. For the experiment, cells were seeded on the glass coverslip or glass bottom dish (Matsunami) coated either 100 µg mL^{-1} (poly-D-lysine; sigma) and 10 µg mL^{-1} of laminin (Wako Pure Chemical Industries), and cultured in Neurobasal Medium (Thermo Fisher Scientific) containing B-27 supplement (Thermo Fisher Scientific) and GlutaMAX™ 100X (Thermo Fisher Scientific). Neurons were treated with 2.5 µM cytosine-β-D-arabinofuronaside after day in vitro (DIV) 3 and then cultured neurons were continued to be incubated at 37°C, 5% CO_2 to DIV 7 and DIV14.

2.3 Transfection

For DIV 7 observation, neurons were transfected with vectors using Nucleofector (Lonza) before plating. Neurons were suspended in 100 µL of Nucleofector™ solution for every 1.0 x 10^6 cells. Vectors were then added into the suspension, mixed well, and transferred into an electroporation cuvette. Using an electroporator (Amaxa Biosystems),

neurons were electroporated to introduce the plasmid DNA into the cells. Immediately after electroporation, cells suspension was transferred to Neurobasal Medium supplemented with 10% fetal bovine serum and 0.01% penicillin streptomycin.

For DIV 14 observation, neurons were transfected at DIV 7 via lipofectamine 2000 according to the manufacture`s protocol (Life Technologies). Briefly, a typical transfection mixture for one 24 well-plate well contained 50 µl Neurobasal medium, 2 µl of lipofectamine solution and 1 µg DNA.

2.4 RNAi

For RNAi experiments, Block-iT Pol II miR RNAi expression kit (Invitrogen) were used to facilitate the expression of microRNA (miRNA). The vectors were transfected into the cultured neurons with lipofectamine 2000 at DIV 4, according to the manufacture's protocol (Invitrogen). Expression of shootin1 was suppressed using shootin1 miRNA#1 (5'-TGAAGCTGTTAAGAAACTGGA-3') and shootin1 miRNA#2 (5'-GTTAGAGGAACGGCTAGAGAA-3') corresponding to nucleotides 138-158 and nucleotides 867-887 in the coding region of rat shootin1, respectively. For control vector shootin1 pcDNA 6.2-GW/EmGFP-miR-neg encodes an mRNA not to target any known vertebrate genes (Toriyama et al., 2006; Toriyama et al., 2013). After 14 days culture, immunocytochemical analyses for PSD-95 or synaptophysin and shootin1a was conducted. Signal fluorescent of shootin1a was used to indicate the reduction of shootin1a expression.

2.5 Genotyping

Male and female shootin1 heterozygous mice were mated to obtain shootin1 KO mice. Genomic DNA was isolated tail biopsies of live embryos by NaOH extraction. 1M Tris-hydrochloric acid (Tris-HCl) (pH 8.0) was added and heated at 95°C for 10 min, then centrifuge for 10 min at 15000 rpm in 4°C. Supernatant was used as DNA template. Genotype was determined by PCR with 4 specific primers :

Genotyping F1 (5`-CAGACTGCTACCCACTACCCCCTAC-3`),
Genotyping R1 (5`-CCTAGAGCTGGACAGCGGATCTGAG-3`),
Genotyping F2 (5`-CCCAGAAAGCGAAGGAACAAAGCTG-3`),
Genotyping R2 (5`-ACCTTGCTCCTTCAAGCTGGTGATG-3`).

The PCR was carried out with the denaturation step at 94°C for 2 min, followed by 30 cycles of 98°C for 10 sec, 60°C for 30 sec, 68°C for 30 sec and a final extension step at 72°C

for 2 min. After the PCR reaction, samples were electrophoresed in 1.2% (w/v) agarose gel at 100V for 20 min. For visualization of electrophoresed PCR products, gels were stained with 0.5 μg/mg of Ethidium bromide for 15 min, washed with milliQ and digital images were captured in a GelDoc-It® Imaging System (UVP).

2.6 Immunocytochemistry and microscopy

Cultured neurons were fixed with 3.7% formaldehyde dissolved in Krebs buffer for 10 min at room temperature, followed by treatment with 0.05% triton X-100 in PBS for 15 min on ice and blocked 10 % fetal bovine serum in PBS for 1h at room temperature. They were then incubated using the following primary antibodies diluted with blocking serum: rabbit anti-shootin1a (1:2000), rabbit anti-shootin1b (1:20000), mouse anti-cortactin (1:500) (Millipore), goat anti-NCAM-L1 (1:500) (Santa Cruz Biotech), mouse anti-PSD-95 (1:500) (Thermo-scientific), mouse anti-synaptophysin (1:500) (Santa Cruz Biotech), mouse anti-myc (1:500) (MBL) or rabbit anti-GFP (1:500) (MBL) overnight at 4^{o}C. Neurons were then washed in PBS and incubated with secondary antibodies conjugated with Alexa Fluor 488 (1:1,000) (Invitrogen). Alexa Fluor 594 (1:1,000) (Invitrogen) for 1 h at room temperature and Alexa Fluor 350-conjugated phalloidin (1:50) (Invitrogen) for 30 min at room temperature. Immunostained cells were mounted with 50% (v/v) glycerol (Nacalai Tesque) in PBS. Fluorescence images were acquired using either a fluorescence microscope (Axioplan2; Carl Zeiss Inc.) equipped with a plan-Apochromat 63× oil, 1.40 NA objective (Carl Zeiss, Inc.), a charge-coupled device camera (CCD, AxioCam MRm, Carl Zeiss) and imaging software (Axiovision3, Carl Zeiss), or a TIRF microscope (IX81, Olympus) and imaging software (MetaMorph, molecular devices).

2.7 Immunoblotting

Lysates of 1 x 10^6 hippocampal neurons from various developmental stages were loaded onto 10% (w/v) SDS-polyacrylamide gel, transferred to PVDF membrane (Shimada et al., 2008; Toriyama et al., 2006). The protein expression was detected using the following antibodies: rabbit anti-shootin1a (Baba et al., 2018) (1:10000), rabbit anti-shootin1b (Higashiguchi et al., 2016) (1:20000), rabbit anti-pSer249-shootin1 and rabbit anti-pSer101-shootin1 (Toriyama et al., 2006; Toriyama et al., 2013) (1:5000 and 1:1000, respectively), mouse anti-actin (1:10000, Millipore). The following secondary antibodies were used in immunoblotting: HRP-conjugated donkey anti-rabbit IgG (1:2000, GE Healthcare) and HRP-conjugated goat anti-mouse IgG (1:5000, Thermo Fisher Scientific). Immunodetection was performed by using the enhance chemiluminescence system (ECL, Amersham, Bioscience).

Chemiluminescent signals were projected on X-ray film and digitalized, and the signals were quantified by using ImageJ.

2.8 DiI staining

Prior to surgery, postnatal (P12) wildtype or shootin1-KO mice were anesthetized with pentobarbital sodium mixture via intraperitoneal (IP) injection. Mice then were perfused with cold PBS buffer and 4% paraformaldehyde (PFA). After perfusion was succeeded, mice head was removed by scissor. Brain was removed gently and immersed in the 4% paraformaldehyde as fixative solution, 4^{o}C for overnight. After 24 hours, serial coronal section (200 μm) of agarose-embedded brains were cut with on a vibrotome (Leica) and collected in PBS. Under dissecting microscope, 1,1`-dioctadecyl-3,3,3`,3`-tetramethyl-indocarbocyanine dye (DiI; Invitrogen) crystals were placed in using a borosilicate glass micropipette with sharp and elongated tip. DiI crystals adhered on the surface of pipette tip were gently delivered to the surrounding hippocampus part of slice section. Section were then preincubated in 1.5% PFA at room temperature for 4-12 hours to allow DiI crystals to fully diffuse along the neuronal membrane of CA1 pyramidal neurons. Slices were then fixed with 4% PFA at room temperature for 30 minutes and mounted in 30% sucrose. Fluorescence images were acquired using confocal microcope (LSM 710; Carl Zeiss) equipped with a plan Apochromat x100, 0.45 NA (Carl Zeiss).

2.9 Fluorescent speckle imaging

For fluorescent speckle imaging experiment, neurons were transfected with HaloTag-actin, HaloTag-shootin1a or HaloTag-cortactin vectors and cultured until DIV 7 on glass bottom dish coated with PDL and laminin. Prior to observation, neurons were treated with HaloTag TMR ligand (Promega) at 1:2000 dilution in the culture medium and incubated for 1 h at 37^{o}C. The ligand was then washed out with PBS and the cells were incubated in L-15 medium containing 2% B27 supplement and GlutaMAX 100X. The fluorescent speckles of HaloTag proteins (actin, shootin1a, or cortactin) were observed using fluorescence microscope (AxioObserver Z1, Carl Zeiss) equipped with a complementary metal oxide semiconductor camera (CMOS, ORCA Flash4.0 V2, Hamamatsu), a Plan-Apochromat 100x, 1.40 NA (Carl Zeiss) and imaging software (ZEN 2012, Carl Zeiss). Fluorescence images were acquired every 2 sec for 100 sec.

2.10 Traction force microscopy

Polyacrylamide gels with embedded fluorescent microsphere (100 nm diameter; Invitrogen) were prepared as described (Toriyama et al., 2013; Abe et al., 2018). Neurons were cultured on PDL-laminin-coated acrylamide gel and incubated at 5%CO_2, 37ºC incubator for 7 days. Time lapse imaging of fluorescent beads and filopodia-like spines was performed at 37ºC using confocal microscope (LSM710; Carl Zeiss) equipped with a C-Apochromat 63x/1.2 W Corr objective. The transfected neurons were determined by EGFP fluorescence or from DIC images. Traction forces under the filopodia-like spines were monitored by visualizing force-induced deformation of the elastic substrate, which is reflected by displacement of the beads from their original positions. The force vectors detected by the beads under individual filopodia-like spines were then averaged. To compare the force under different conditions, the length of beads displacement (μm) and angle (θ) of the force vectors of the individual filopodia-like spines were statistically analyzed and expressed as means ± SEM, separately (Toriyama et al., 2013; Abe et al., 2018).

2.11 Chemical LTP

NMDAR-dependent chemical LTP was induced by 200 μM glycine application in Mg^{2+} -free extracellular solution according to Hruska et al., (2018). DIV 14 hippocampal neurons transfected with pEGFP were incubated in artificial cerebrospinal fluid (ACSF, 143 mM NaCl, 5 mM KCl, 2 mM $CaCl_2$, 1mM $MgCl_2$, 30 mM glucose and 10 mM HEPES, pH 7.4) containing 0.5 μM TTX, 1 μM strychnine and 20 μM bicuculline. After 15-30 min of imaging, cultures of neurons were stimulated with glycine (143 mM NaCl, 5 mM KCl, 2 mM $CaCl_2$, 0 mM $MgCl_2$, 30 mM glucose and 10 mM HEPES, pH 7.4, 0.5 μM TTX, 1 μM strychnine, 20 μM bicuculline and 200 μM) for 4 min. Cells were then incubated in 0 mM $MgCl_2$ containing ACSF. To block cLTP, 50 μM D-AP5 (D-2-amino-5-phosphonovalerate) and 10 μM of MK-801 were included in the solution described above. Time lapse imaging was conducted every 5 min for 1 h at 37ºC in confocal microscope (LSM 710; Carl Zeiss). Spines were classified as enlarged only if their size increased at least 10% immediately following the application of glycine and remained elevated (≥ 10% over baseline) for the entire imaging period.

2.12 Analyses of dendritic spine morphology

Images were acquired using a confocal microscope (LSM710; Carl Zeiss) with consistent laser intensity or camera exposure levels for each fluorophore in each experiment. Dendritic segments of interest in hippocampal neurons were first taken as three-dimensional

image stacks and then projected to two-dimensional images using the maximal intensity-z projection function of ImageJ (National Institute of Health). Morphological analysis was performed with ImageJ to measure spine density and size. For each dendritic spines, the length, the neck and head width were measured, which was to classify spines into categories (Filopodia-like, thin, stubby and mushroom-shaped) (Harris et al., 1992; Risher et al., 2014). "Filopodia-like spines" were defined if the length value is ≥ 2 μm and diameter of the head is similar with the neck diameter; "Thin" spine with ≤ 5 μm in length, and diameter head ≤ 0.6 μm; "Stubby" spine with ≤ 2 μm in length, without a well-defined neck; "Mushroom-shaped" spine is ≤ 5 μm in length and head diameter much bigger than neck diameter with value ≥ 0.6 μm.

2.13 Statistical analysis

All statistical significance was determined by Microsoft Excel and GraphPad Prism7 (RRID : SCR_002798). For the most cases, significance was determined by two-tailed unpaired Student's *t*-test.

3. Results

3.1 Shootin1a is localized in dendritic spines

Previous studies reported that shootin1a is expressed at early stages of developmental hippocampal neurons and have shown that shootin1a is predominantly accumulated at the axonal growth cone (Toriyama et al., 2006). Shootin1a is involved in the process of neuronal polarity formation and axon guidance (Toriyama et al., 2010; Kubo et al., 2015; Baba et al., 2018). To address whether shootin1a is expressed in the later stages of developmental hippocampal neurons, cell lysates from rat cultured hippocampal neurons on day in vitro (DIV) 3, DIV 7, DIV 14, and DIV 28 were analyzed by immunoblotting. In addition, I also examined the expression level of another splicing isoform of shootin1a, shootin1b (Higashiguchi et al., 2016). Immunoblot was conducted by using specific antibodies against shootin1a and shootin1b. The level of actin served as a loading control. The results showed that the expression level of shootin1a increased remarkably on DIV 7. Thereafter, it decreased but still was detected on DIV 14 and DIV 28 (Figure 5A). On the other hand, shootin1b was detected on DIV 3, thereafter decreased on DIV 7 and became undetectable on DIV 14 and DIV 28 (Figure 5A). These data suggest that shootin1a, but not shootin1b, is expressed at later stages of developmental hippocampal neuron and raised the possibility that shootin1a may function at the later stages of developmental hippocampal neurons.

The peak of dendritic growth and synapse formation of cultured hippocampal neurons occurs during the second and third weeks *in vitro* (Kaech and Banker, 2006). To examine whether shootin1a is localized in dendritic spines, I performed immunocytochemical analysis of DIV 14 hippocampal neurons. Neurons were double-stained by anti-shootin1a or anti-shootin1b antibodies with a dendritic spine marker, anti-PSD-95 antibody. As shown in Figure 5B, shootin1a was detected and was co-localized with PSD-95 positive puncta. In addition, consistent with immunoblot data, shootin1b was not detected in the spines. The immature forms of dendritic spines, filopodia-like and thin spines, are observed at the younger neurons, DIV 9-12 (Ziv and Smith, 1996). Thus, I examined the subcellular localization of shootin1a in the immature spines at DIV 12 cultured hippocampal neurons. To outline the morphology of dendritic spines, neurons were transfected with AcGFP-actin using Lipofectamine 2000 and then labeled with anti-shootin1a antibody. As shown in Figure 5C, endogenous shootin1a localized at the tips of filopodia-like spines (arrowheads) and stubby spines (arrows). Previous study reported that elongated morphology of filopodia-like spines

serve as precursors of dendritic spine (Ziv and Smith, 1996). Together, these data demonstrate that shootin1a is detected in dendritic spine sand localized at the tips of filopodia-like spines.

3.2 Shootin1a is involved in dendritic spine formation

To elucidate the role of shootin1a in dendritic spines, I analyzed the neuron of shootin1 knock out mice (Baba et al., 2018) *in vitro* and *in vivo*. First, Hippocampal neurons were isolated from E16.5 wild-type (WT) and shootin1-KO mice at E16.5 and then cultured at low-density. On DIV 14, neurons were double-stained with anti-shootin1a antibody and anti-PSD-95 antibody (Figure 6A). As the result, shootin1-KO neurons exhibited a significantly low number of PSD-95-positive puncta compared with those in WT neurons (Figure 6B; WT, 2.61 ± 0.19 puncta/10 μm, n = 37 cells; KO, 1.51 ± 0.12 puncta/10 μm, n = 38 cells). Additionally, shootin1-KO neurons showed a decreased number of synaptophysin-positive puncta (Figure 6C), a presynaptic protein marker (Figure D; WT = 3.13 puncta/10μm, n = 30 cells; shootin1-KO = 1.46 puncta/10μm, n= 43 cells). The graph depicts the averaged result from more than 3 experiments.

Shootin1a plays an important role for axon outgrowth and guidance (Toriyama et al., 2006; Abe et al., 2018; Baba et al., 2018). Thus, reduction of the dendritic spine number in shootin1-KO neurons might be induced as an indirect effect of axon outgrowth inhibition. Therefore, I transfected DIV 4 low-density cultured E18 rat hippocampal neurons using miRNA against shootin1 that specifically knockdowns rat shootin1a. Transfection efficiency was around 1.6% - 2% on DIV 14 hippocampal neurons (Figure 7B), suggesting that axon outgrowth of 98% neurons are not affected. Neurons were then stained with anti-PSD-95. The fluorescence of GFP indicated transfected neurons (Figure 7A). The result showed that transfected GFP-positive neurons silenced for shootin1a presented a significant reduction of PSD-95-positive puncta compared with control (Figure 7C; control shootin1a-RNAi, 2.20 ± 0.09 puncta/10 μm, n = 22 cells; shootin1a RNAi #1, 1.65 ± 0.09 puncta/10 μm, n = 18 cells; shootin1a RNAi #2, 1.78 ± 0.08 puncta/10 μm, n = 10).

To further examine the role of shootin1a, I over expressed myc-shootin1a in cultured hippocampal neurons under strong β-actin promotor (Figure 8A). Overexpression of shootin1a in cultured hippocampal neurons increased the density of PSD-95 immunoreactivty (Figure 8B; control = 2.28 ± 0.09 puncta/10μm, n = 21 cells; shootin1a overexpressing neurons = 2.85 ± 0.11 puncta/10μm, n = 21 cells). Together, these results demonstrate that shootin1a plays an important role for dendritic spine formation.

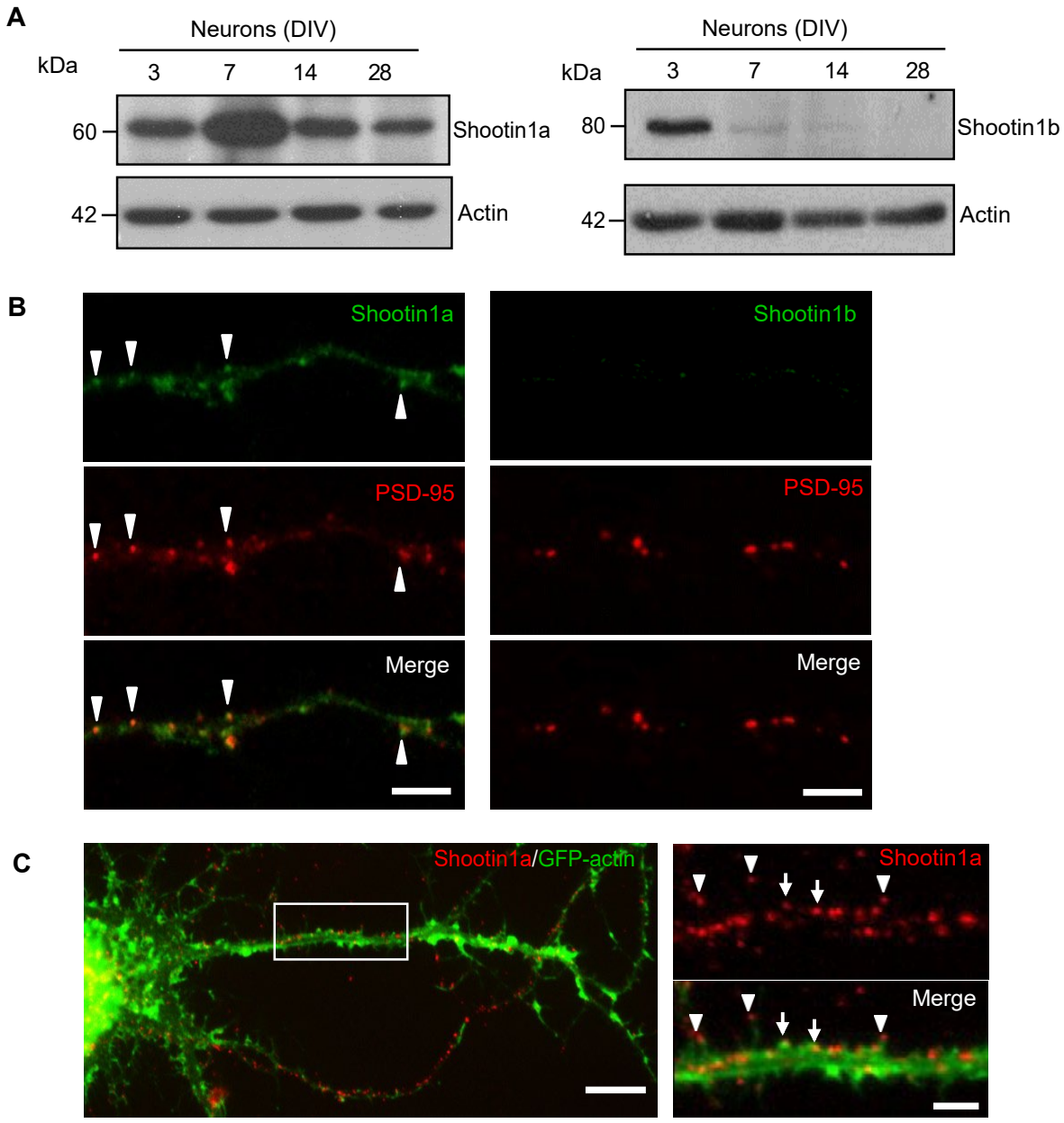

Figure 5. Expression and localization of shootin1a in dendritic spines. (A) Immunoblot analysis of shootin1a and shootin1b on DIV 3, 7, 14 and 28 of E18 rat hippocampal neurons. The anti-shootin1a (~60 kDa) and anti-shootin1b (~80 kDa) antibodies recognized specifically shootin1a and shootin1b, respectively. Anti-actin antibody served as loading controls. (B) DIV 14 primary hippocampal neurons were immunostained for endogenous shootin1a or shootin1b (green) and PSD-95 (red). PSD-95 is a marker for dendritic spines. Arrowheads indicate shootin1a co-localized with PSD-95. Bars, 5 μm. (C) DIV 10 neurons transfected with AcGFP-actin were immunostained with shootin1a (red). Arrowheads indicate shootin1a localized at the tips of filopodia-like spines, while arrows indicate shootin1a localized in a stubby spines. Bars, 10 μm; 2 μm.

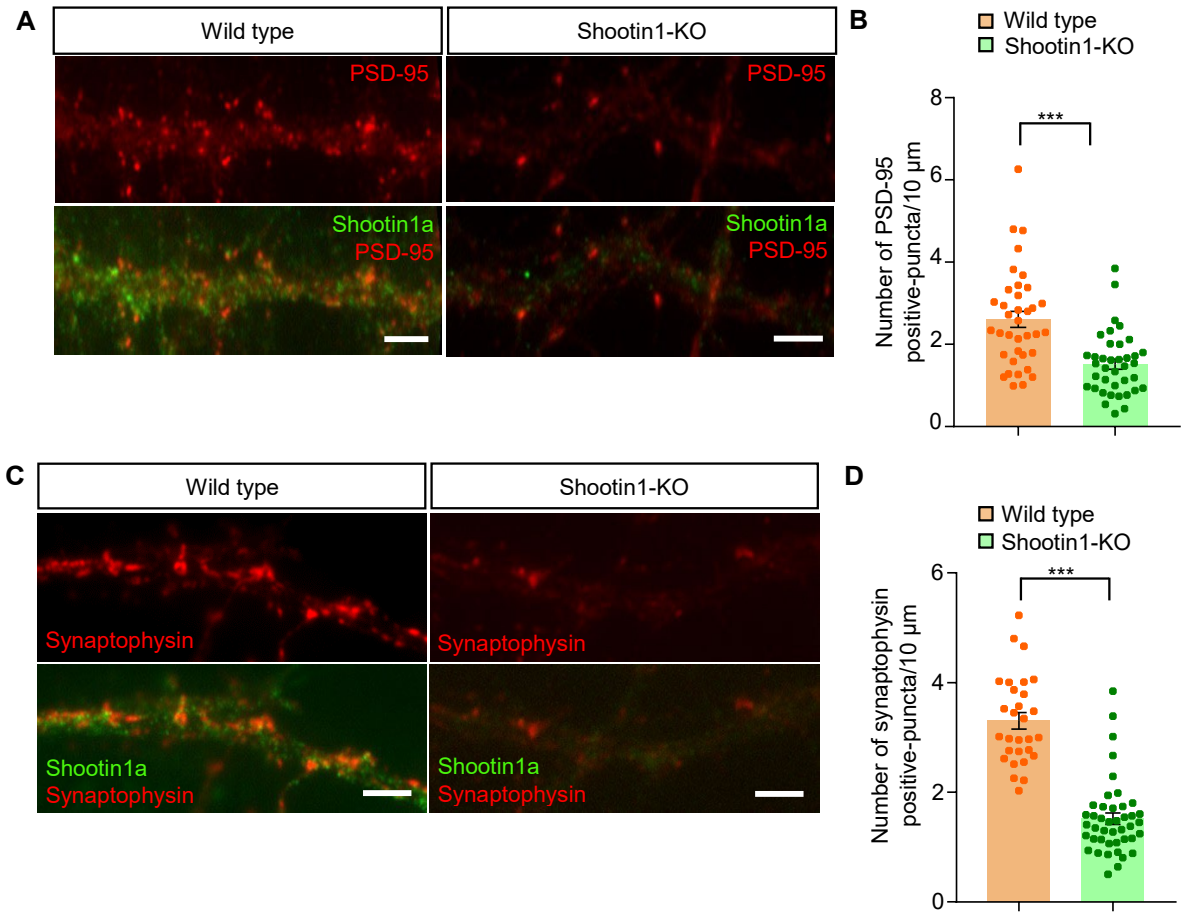

Figure 6. Loss of shootin1a inhibits dendritic spine formation. (A) Immunocytochemical analyses of PSD-95-positive puncta in E16.5 WT and shootin1-KO mouse hippocampal neurons cultured for 14 days. (B) Quantitative analyses of PSD-9-positive puncta number. Density of PSD-95-positive puncta: wt = 2.61 puncta ± 0.19/10µm, n = 37 cells; shootin1-KO = 1.52 ± 0.12 puncta/10µm, n = 38 cells. (C) Immunocytochemical analysis of synaptophysin-positive puncta in E16.5 WT and shootin1-KO mice neurons cultured for 14 days. (D) Quantification analyses of synaptophysin-positive puncta. Density of Synaptophysin-positive puncta: wt = 3.13 puncta/10µm, n = 30 cells; shootin1-KO = 1.46 puncta/10µm, n= 43 cells. Two-tailed unpaired Student's t-test. *p < 0.05; **p < 0.02; ***p < 0.01. Scale bars, 5 µm

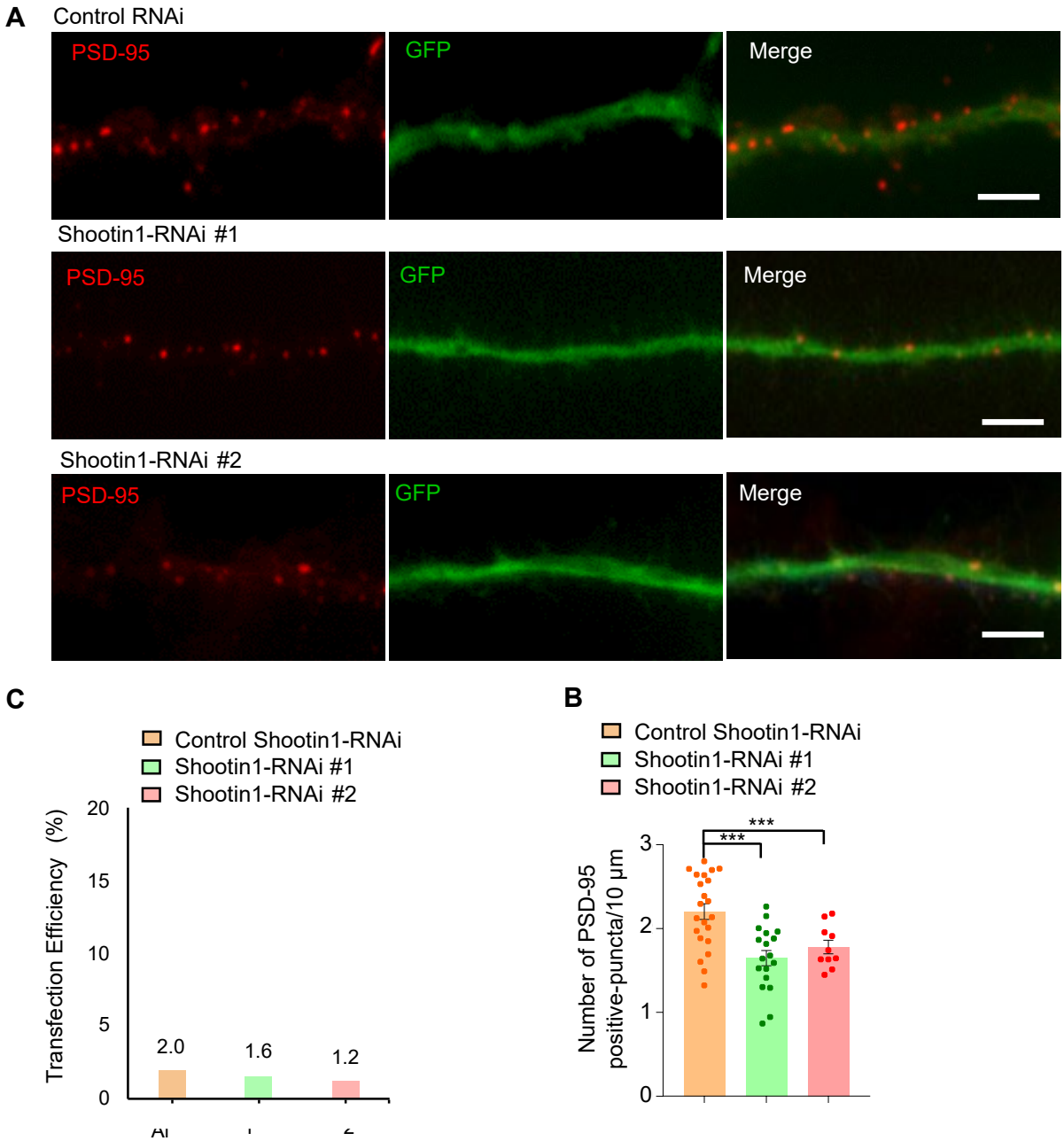

Figure 7. **Shootin1a-knockdown neurons show a low number of dendritic spines.** (A) Immunocytochemical analyses of PSD-95-positive puncta in E18 Rat hippocampal neurons expressing control miRNA and shootin1-RNAi #1 and #2. (B) Transfection efficiency of Lipofectamine 2000 in DIV 14 hippocampal neurons. Neurons were transfected on DIV 4 and then on DIV 14 observation was performed. (C) Quantification of the spine number in shootin1-knockdown neurons. Density of PSD-95-positive puncta: control shootin1a-RNAi = 2.20 puncta ± 0.09/10µm, n = 22 cells; shootin1-RNAi #1 = 1.65 ± 0.09 puncta/10µm, n = 18 cells; shootin1-RNAi #2 = 1.78 puncta ± 0.08/10µm, n = 10 cells. Two-tailed unpaired Student's t-test. *p < 0.05; **p < 0.02; ***p < 0.01. Scale bars, 5 µm.

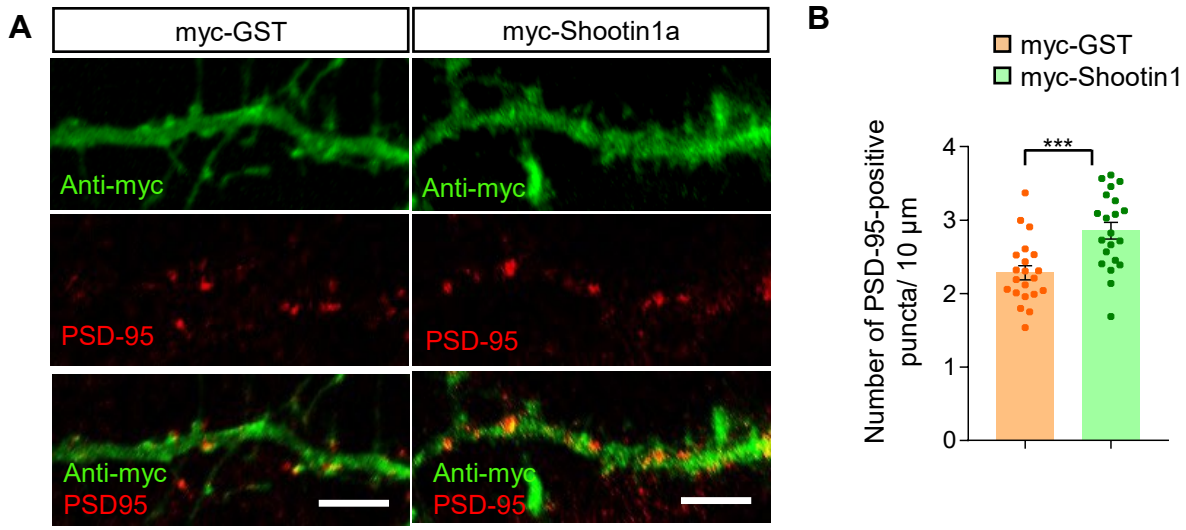

Figure 8. Overexpression of shootin1a increases PSD-95-positive puncta. (A) Overexpression of shootin1a in DIV 14 hippocampal neurons. Hippocampal neurons overexpressing myc-GST or myc-shootin1a were immunostained with anti-myc (green) and anti-PSD-95 (red) antibodies. (B) Quantification of the spine number in P12 WT and shootin1-KO mice brain. Density of PSD-95-positive puncta: myc-GST neurons= 2.28 puncta ± 0.09/10µm, n = 21 cells; myc-shootin1 neurons = 2.85 ± 0.11 puncta/10µm, n = 21 cells. Two-tailed unpaired Student's test; ***p < 0.01. Bars, 5 µm.

3.3 Shootin1a is involved in the maturation of dendritic spines

To further examine the role of shootin1a *in vivo*, the carbocyanine dye DiI was delivered to the hippocampus of P12 WT and shootin1-KO mice brain. During P10-P12, immature filopodia-like spines are replaced with mature spines (Cruz-Martin et al., 2010). Distinctive morphologies such as dendritic branches and dendritic spine protrusions could be visualized under confocal microscope (Figure 9A). Consistent with the number of PSD-95-positive puncta in shootin1-KO neurons in culture, dendritic spine number of pyramidal hippocampal neurons in shootin1-KO mice brain was significantly decreased compared with WT (Figure 9B; WT, 4.50 ± 0.37 protrusions/10 μm, n = 10 cells; KO, 3.51 ± 0.22 protrusions/10 μm, n = 11 cells).

To address whether shootin1a is involved in spine maturation, DiI staining images were also used for discriminating the spine morphology. Spine morphology was categorized as previously described with some modifications (Harris et al., 1992; Risher et al., 2014) : "filopodia-like spines" if the length value is ≥ 2 μm and diameter of the head is similar with the neck diameter; "Thin" spine is ≤ 5 μm in length, and diameter head is ≤ 0.6 μm; "Stubby" spine is ≤ 2 μm in length, without a well-defined neck; "Mushroom-shaped" spine is ≤ 5 μm in length and head diameter much bigger than neck diameter with value ≥ 0.6 μm. As shown in Figure 9C, in shootin1-KO mice brain, the density of filopodia-like spines increased (Filopodia-like spines: WT, 6.18 ± 0.79 %, n = 10 cells; KO, 13.73 ± 2.42 %, n = 11 cells), while mushroom-shaped spines number decreased compared with WT (WT, 38 ± 3.59 %, n = 10 cells; KO, 28.55 ± 2.53 %, n = 11 cells). The numbers of thin and stubby spines were not significantly different between shootin1-KO and WT. These data demonstrate that shootin1a is involved in the maturation of dendritic spines.

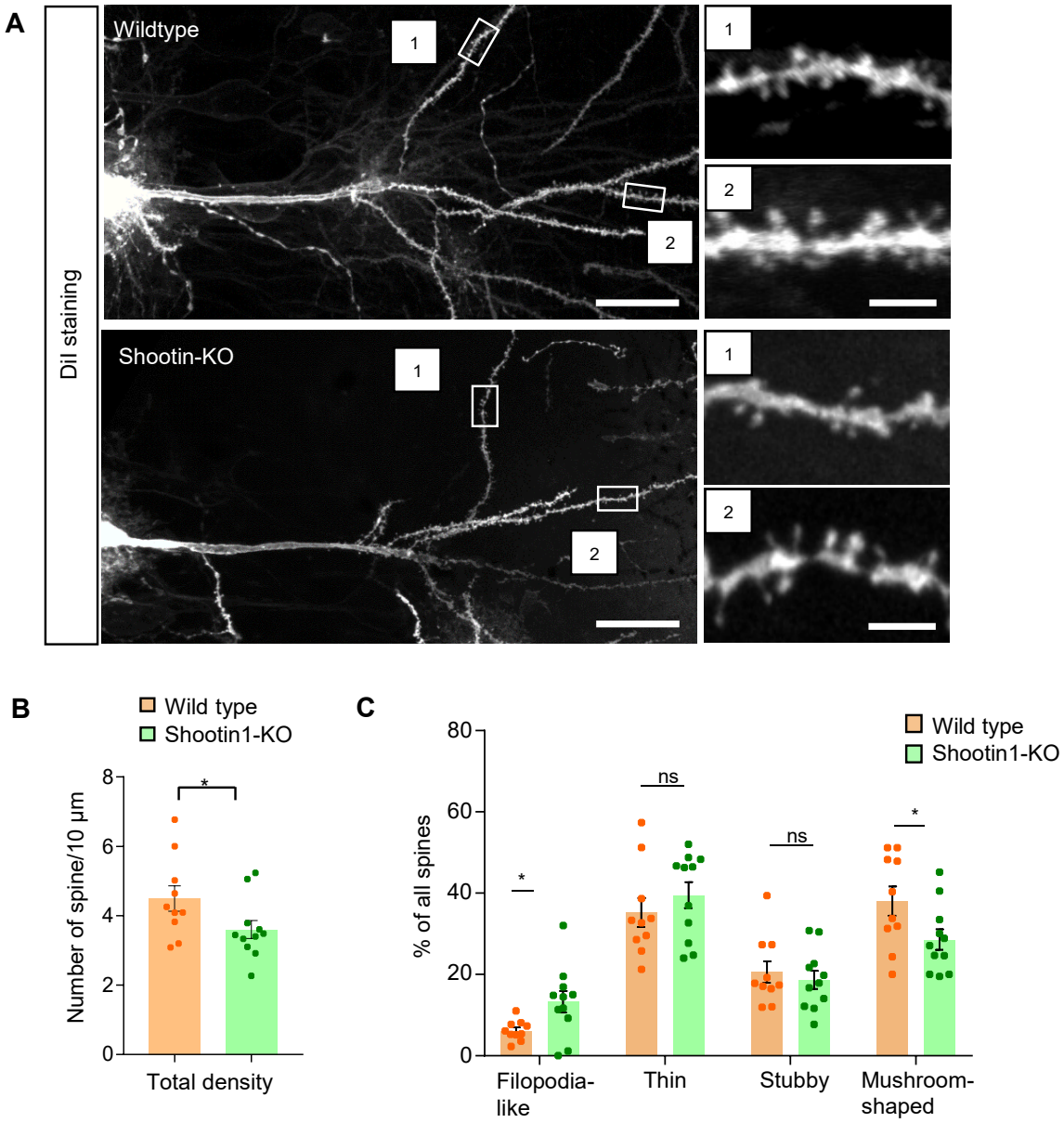

Figure 9. Shootin1a is required for the maturation of dendritic spines. (A) Representative images of DiI-stained dendritic shaft in P12 WT and shootin1-KO mice brain. (B) Quantification of the spine number in P12 WT and shootin1-KO mice brain. Number of spines: WT, 4.50 ± 0.37/10 µm, n = 10 cells; KO, 3.51 ± 0.22/10 µm, n = 11 cells. Two-tailed unpaired Student's test; *p < 0.05. (C) Proportion of filopodia-like, thin, stubby and mushroom-shaped spines in P12 WT and shootin1-KO mice brain. Filopodia-like: WT, 06.18 ± 0.79 %; KO, 13.73 ± 2.42 %; thin spines: WT, 35.21 ± 3.55 %; KO, 39.50 ± 3.19 %; stubby spines: 20.59 ± 2.67 %; KO, 18.66 ± 2.23 %; mushroom-shaped: 38.01 ± 3.59 %; KO, 28.55 ± 2.53 %; n WT = 10 cells, n KO = 11 cells). Two-tailed unpaired Student's test; *p < 0.05; ns, non significant. Bars, 20 µm; 5 µm.

3.4 Shootin1a mediates clutch coupling at dendritic spines

Previously, our laboratory reported that shootin1a functions as a clutch molecule for axon outgrowth and guidance (Shimada et al., 2008; Kubo et al., 2015; Baba et al., 2018). At axonal growth cones, shootin1a interacts with F-actin retrograde flow, through its interaction with cortactin (Kubo et al., 2015) and L1-CAM (Baba et al., 2018). Therefore, to investigate whether shootin1a functions as a clutch molecule for spine formation, I first analyzed localization of F-actin, shootin1a, and L1-CAM in filopodia-like spines of DIV 7 hippocampal neurons. I found that shootin1a was accumulated at the tips of filopodia-like spines and it was co-localized with F-actin, cortactin and L1-CAM (Figure 10).

To further investigate whether shootin1a functions as a clutch molecule in dendritic spines, I carried out single speckle imaging of HaloTag-actin, HaloTag-shootin1a and HaloTag cortactin. The protein tag (HaloTag) system allows to select the type of ligand for multiple analytical methods including analysis of subcellular localization (Los et al., 2008). In this study, F-actin, cortactin, or shootin1a were fused to HaloTag and were labeled by tetramethylrhodamine (TMR) to visualize the dynamics of those proteins. The flow velocity was monitored by a kymograph analysis. A previous study reported that retrograde flow movement of F-actin in filopodia-like spine of DIV 7-9 cultured hippocampal neurons (Tatavarty et al., 2012). Consistently, I found that fluorescent speckles of F-actin moved retrogradely in filopodia-like spines of DIV 7 hippocampal neurons (Figure 11A). Similarly, fluorescent speckles of shootin1a and cortactin also showed retrograde movement (Figure 11B and C). These data raise a possibility that shootin1a mechanically couples F-actin and adhesive substrate in dendritic spines. Previous studies reported that disruption of the shootin1a-mediated clutch coupling between retrograde flow of F-actin and substrate increases the speed of F-actin retrograde flow (Toriyama et al., 2013; Kubo et al., 2015; Baba et al., 2018). Interestingly, the flow speed of HaloTag-actin speckles was significantly increased in shootin1-KO neurons (Figure 12; shootin1-WT, 1.96 ± 0.12 μm min^{-1}, n = 66 speckles; shootin1-KO, 3.274 ± 0.23 μm min^{-1}, n = 68 speckles), suggesting that shootin1-KO increased slippage of F-actin-adhesion coupling, namely, shootin1-KO disrupted clutch coupling in dendritic spines. Taken together, these results demonstrate that shootin1a mediates F-actin-adhesion clutch coupling at dendritic spine.

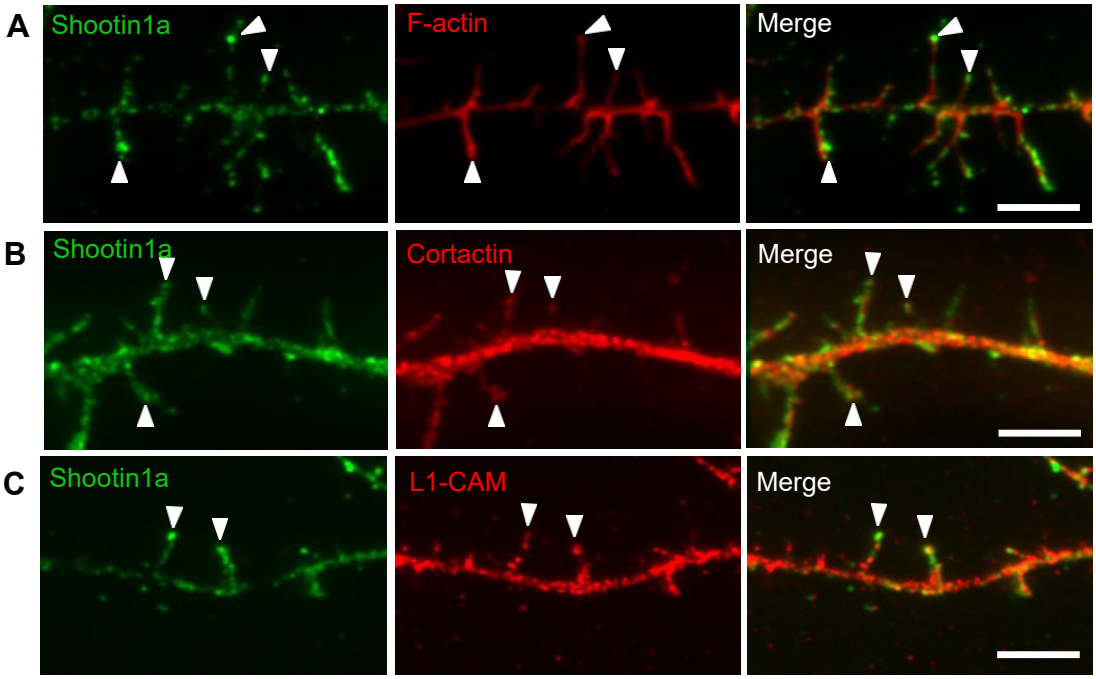

Figure 10. Shootin1a co-localizes with F-actin, Cortactin and L1-CAM. (A-C) DIV 7 primary hippocampal neurons co-stained with anti-shootin1a (green) (A-C) phalloidin for F-actin (A), anti-cortactin antibody (B), and anti-L1-CAM antibody (C). Scale bars, 5 μm.

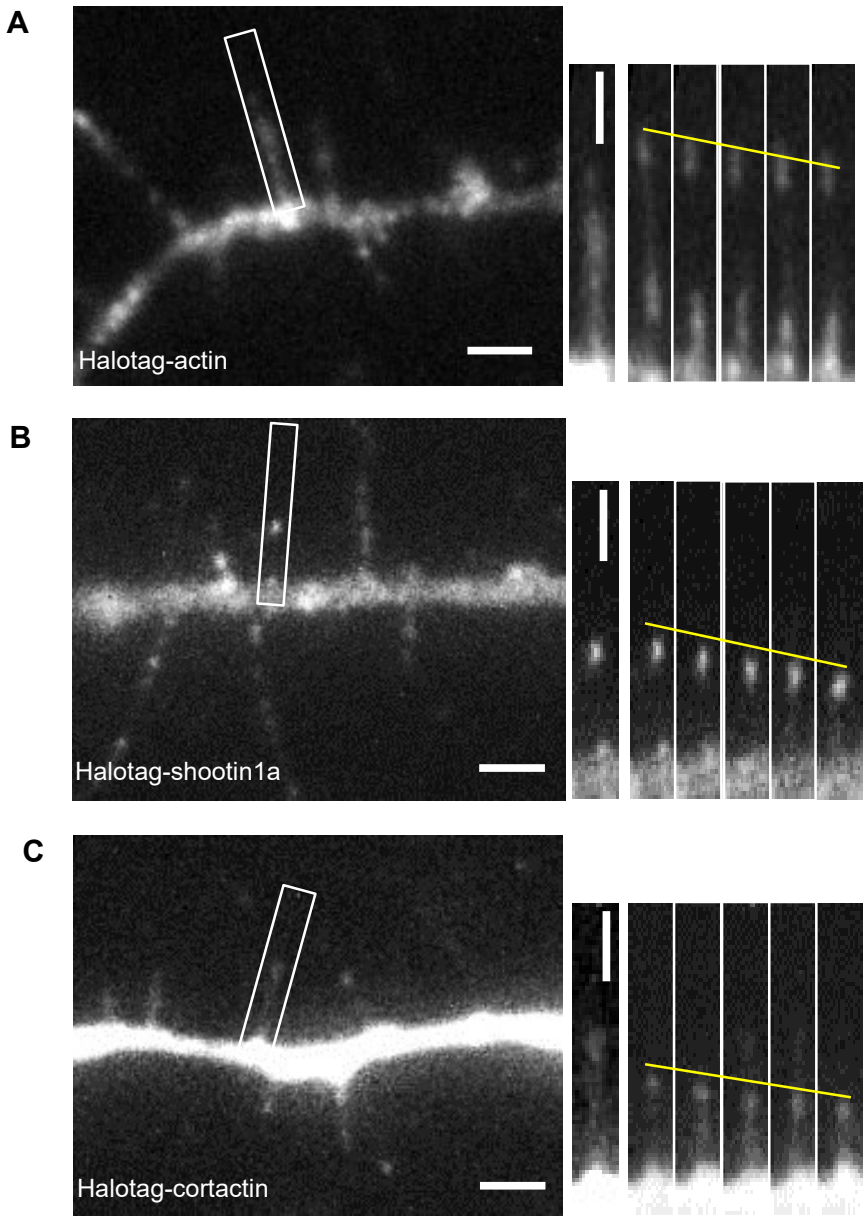

Figure 11. Shootin1a flows retrogradely in filopodia-like spines. (A) Fluorescent speckle images of halotag-actin at filopodia-like spine in DIV 7 hippocampal neurons. Kymograph of the indicated rectangular region at 2-sec intervals is shown to the right. Yellow dashed lines indicate the retrograde flow of halotag-actin. Scale bars, 2 μm ;1 μm. (B) Fluorescent speckle images of Halotag-shootin1a at filopodia-like spine in DIV 7 rat hippocampal neurons. Kymograph of the indicated rectangular region at 2-sec intervals is shown to the right. Yellow dashed lines indicate the retrograde flow of halotag-shootin1a. Scale bars, 2 μm ;1 μm. (C) Fluorescent speckle images of halotag-cortactin at filopodia-like spine in DIV 7 rat hippocampal neurons. Kymograph of the indicated rectangular region at 2-sec intervals is shown to the right. Yellow dashed lines indicate the retrograde flow of halotag-cortactin. Scale bars, 2 μm ;1 μm

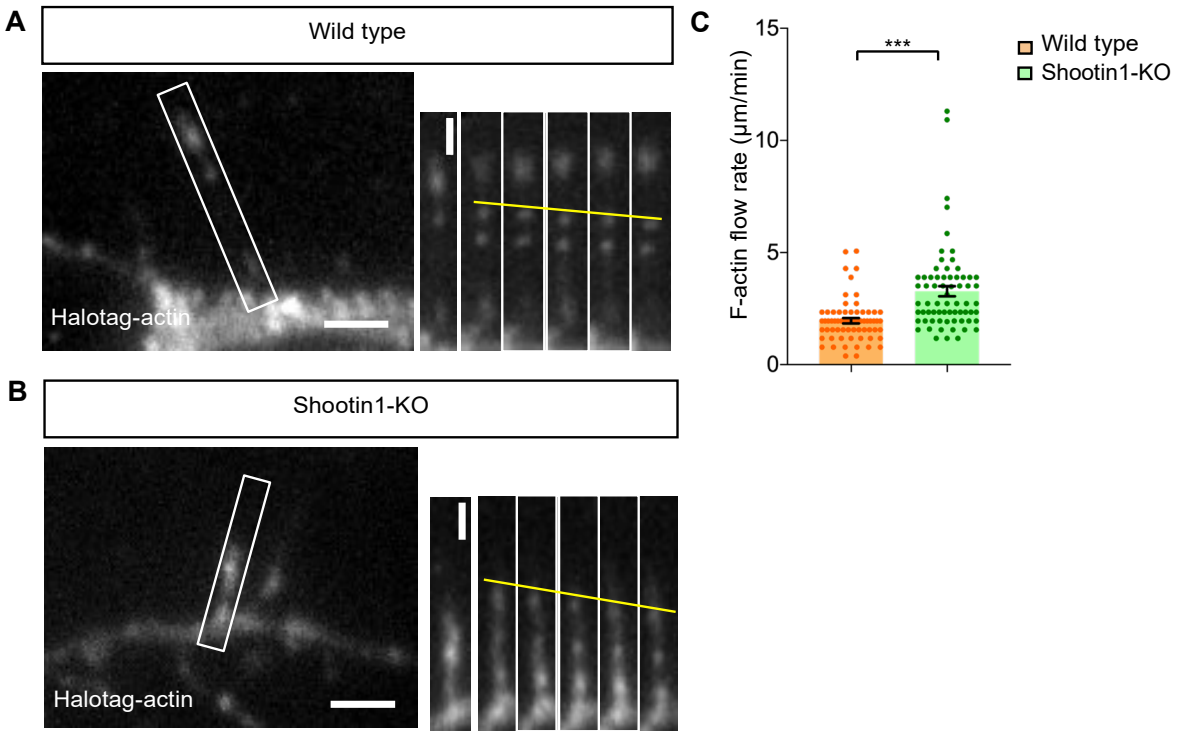

Figure 12. F-actin retrograde flow speeds in filopodia-like spines of WT and shootin1-KO neurons. (A and B) Fluorescent speckle images of halotag-actin in filopodia-like spines of WT and shootin1-KO DIV 7 mice hippocampal neurons. Kymograph of the indicated rectangular region at 2-sec intervals is shown to the right. Yellow dashed lines indicate the retrograde flow of halotag-actin. Scale bars, 2 μm ;1 μm. (C) Quantification of F-actin retrograde flow rate from the kymograph analysis (WT, 1.96 ± 0.12 μm min^{-1}, n = 66 speckles; shootin1-KO, 3.274 ± 0.23 μm min^{-1}, n = 68 speckles). Two-tailed unpaired Student's t-test ***p < 0.01.

3.5 Shootin1a-mediated F-actin-adhesion clutch is involved in dendritic spine formation

To further investigate the roles of shootin1a-mediated F-actin-adhesion clutch for dendritic spines, I overexpressed a shootin1a-dominant negative mutant shootin1a (1-125) in DIV 7 hippocampal neurons. The shootin1a (1-125) is a truncated mutant of shootin1a with residues 1 to 125, which contains the L1-CAM-binding domain but lacks the cortactin-binding domain (Baba et al., 2018). Therefore, the competitive binding of shootin1a-DN to the L1 intracellular domain reduces the binding of endogenous shootin1 to L1-CAM. Consistently with the data of shootin1-KO neurons (Figure 12), the speed of F-actin flow in filopodia-like spines of neurons expressing shootin1a-DN (Figure 13 A and B) was significantly increased compared with control-GST (Figure 13 C; control, 1.89 ± 0.15 μm min^{-1}, n = 40 speckles; shootin1-DN (1-125), 2.59 ± 0.18 μm min^{-1}, n = 55 speckles). These data confirm that interaction of shootin1a and L1-CAM is essential for the clutch coupling of F-actin and adhesive substrate in spines.

The maturation and formation of dendritic spine is primarily driven by the actin network beneath the cell membrane (Honkura et al., 2008; Hotulainen and Hoogenraad, 2010). To examine whether force is generated in dendritic spine, I measured the force by traction force microscopy. Hippocampal neurons were cultured on PDL-laminin-coated acrylamide gel and incubated for 7 days. Traction forces under the spines were monitored by visualizing force-induced deformation of the elastic substrate, which is reflected by displacement of the beads from their original positions. As shown in Figure 14A, the beads moved dynamically under the filopodia-like spines, indicating that force is generated at spines. Importantly, the bead displacement in the neurons expressing shootin1a-DN was significantly decreased in comparison to control neurons (Figure 14B; control, 0.33 ± 0.05 μm, n = 25 spines; shootin1a-DN (1-125), 0.17 ± 0.17 μm, n = 27 spines). The direction of the bead movement was oriented toward the shaft (Figure 14C). These data indicate that disruption of shootin1a-mediated F-actin-adhesion clutch coupling by overexpressing of shootin1a-DN significantly reduce traction force in spines.

I further examined the formation of dendritic spines in neurons expressing shootin1a-DN mutant. DIV 7 hippocampal neurons were transfected with myc-GST or myc-shootin1a (1-125). On DIV 14, neurons were double stained with anti-myc and anti-PSD-95 antibodies to label transfected neurons and dendritic spines, respectively (Figure 15A). As the results, DIV 14 hippocampal neurons transfected with shootin1a-DN (1-125) mutant beared a significantly low number of dendritic spines compared with control (Figure 15B; control, 2.80

± 0.24/10 μm, n = 7 cells; shootin1-DN (1-125), 1.46 ± 0.16/10 μm, n = 12 cells). Together, these results suggest that shootin1a-mediated F-actin adhesion clutch is involved in the generation of traction force for dendritic spine formation.

3.6 Glutamate stimulation elicits Pak1-mediated shootin1 phosphorylation

Glutamate, a major excitatory neurotransmitter, activates postsynaptic glutamate NMDA receptors which in turn induces long-term potentiation (LTP) (Lisman et al., 2012). As a paradigm of learning and memory, a stable enlargement of potentiated spines is associated with LTP (Fortin et al., 2010) and protein phosphorylation is thought to trigger synaptic changes underlying LTP (Racaniello et al., 2010). Therefore, to address whether shootin1a phosphorylation is mediated by glutamate stimulation, I performed immunoblotting for shootin1a phosphorylation at Ser249. As shown in Figure 16, upon stimulation with 10 μM glutamate for 30 min, phosphorylation level of shootin1a at Ser249 was increased significantly (Figure 16).

Previous study reported that netrin-1 induces Pak1-mediated phosphorylation of shootin1a at Ser101 and Ser249 (Toriyama et al., 2013). To determine whether shootin1 phosphorylation is mediated by Pak1 under glutamate stimulation, neurons were treated with a Pak1 inhibitor, NVS-PAK1-1, and stimulated by glutamate. NVS-PAK1-1 is an allosteric inhibitor that binds outside of ATP-binding cleft (non-ATP-competitive Pak1 inhibitor), which selectively inhibits Pak1 kinase activity (Karpov et al., 2015; Semenova and Chernoff, 2017). As the results, under glutamate stimulation, phosphorylation of shootin1a Ser249 was inhibited by NVS-PAK-1-1. These results suggest that glutamate stimulation elicits Pak1-mediated shootin1a phosphorylation.

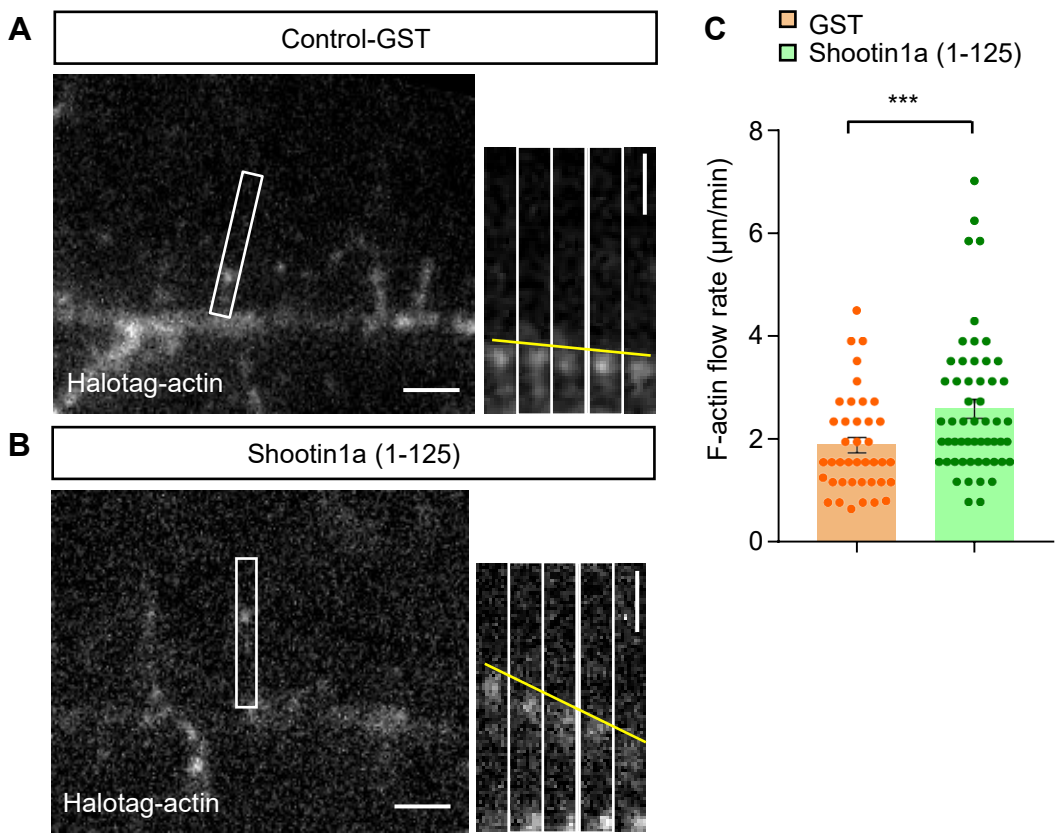

Figure 13. Shootin1a-L1-CAM interaction mediates the clutch coupling of F-actin and adhesive substrates in dendritic spines. (A and B) Fluorescent speckle images of halotag-actin at filopodia-like spines of DIV 7 hippocampal neurons expressing GST (control) (A) and shootin1a (1-125) (B). Kymograph of the indicated rectangular region at 2-sec intervals is shown to the right. Dashed lines indicate the retrograde flow of halotag-actin. (C) Quantification of F-actin retrograde flow rate from the kymograph analysis (control-GST n = 40 Speckles; Shootin1a (1-125) n = 55 Speckles). Two-tailed unpaired Student's t-test ***$p < 0.01$. Scale bars, 2 μm ;1 μm.

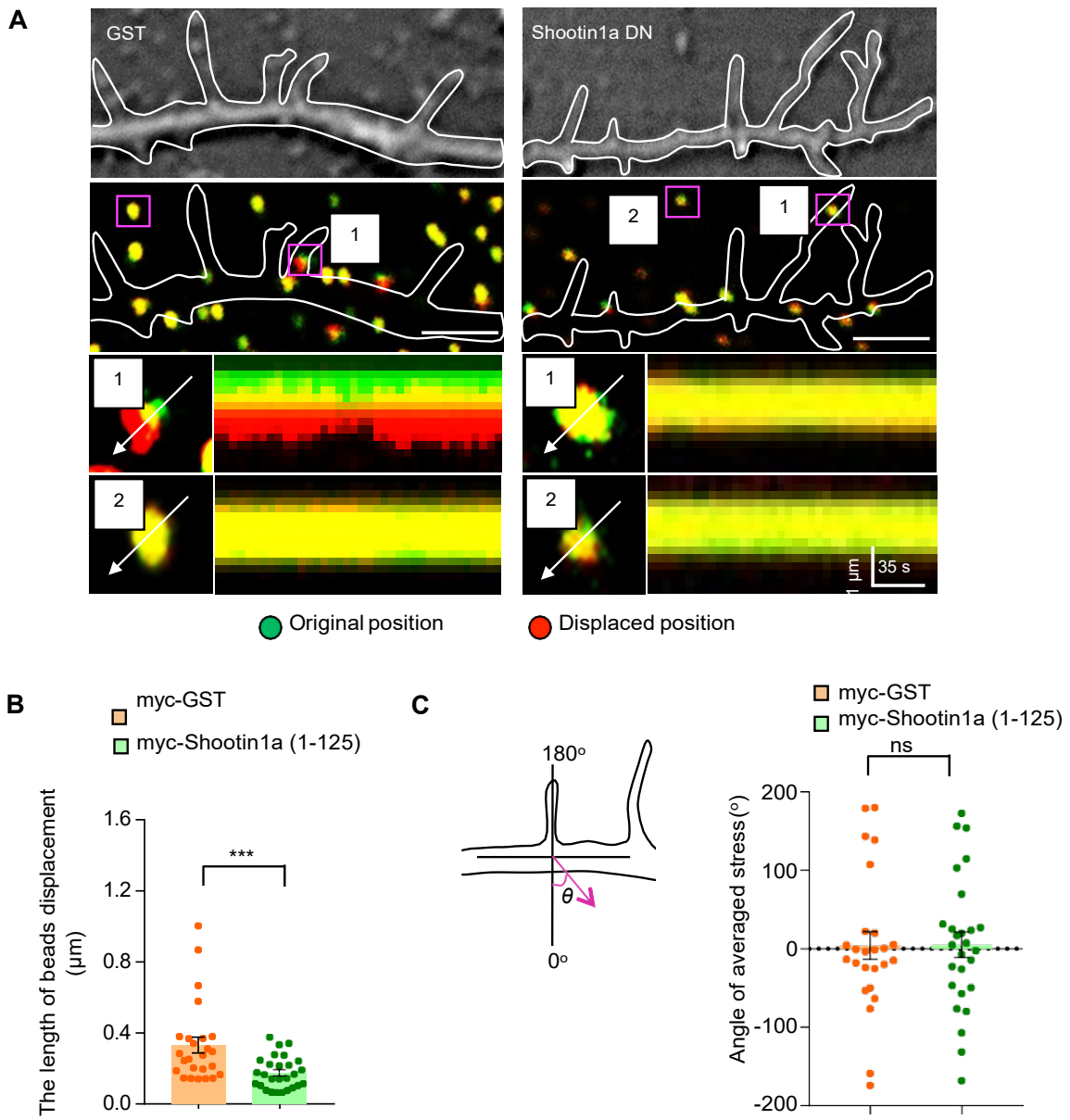

Figure 14. Disruption of shootin1a-mediated F-actin-adhesion clutch inhibits force generation in spines. (A) Analysis of DIC (Upper panel) and fluorescence images (bottom panel) showing filopodia-like spines of DIV 7 neurons overexpressing myc-GST (control) or myc-shootin1a (1-125). Images were acquired every 5 sec. The original and displaced positions of the beads in the gel are indicated by green and red colors, respectively. Dashed line indicates the boundarys of the dendritic shaft with filopodia-like spines. The kymographs (bottom panel) along axis of bead displacement (white dashed arrows) at indicated areas 1 and 2 of the filopodia-like spines show movement of beads recorded every 5 s. The bead in area 2 is reference beads. (B) Quantification of the bead displacement under the filopodia-like spines overexpressing myc-GST (control) (n= 25 beads, 22 spines), myc-shootin1a (1-125) (n= 27 beads, 27 filopodia). (C) Statistical analysis of angle (θ) (myc-GST = 4.221 ± 17.77° ; myc-shootin1a (1-125) = 5.176 ± 16.38°). Two-tailed unpaired Student's *t*-test. ***p < 0.01; ns P = non significant. Scale bars, 5 μm.

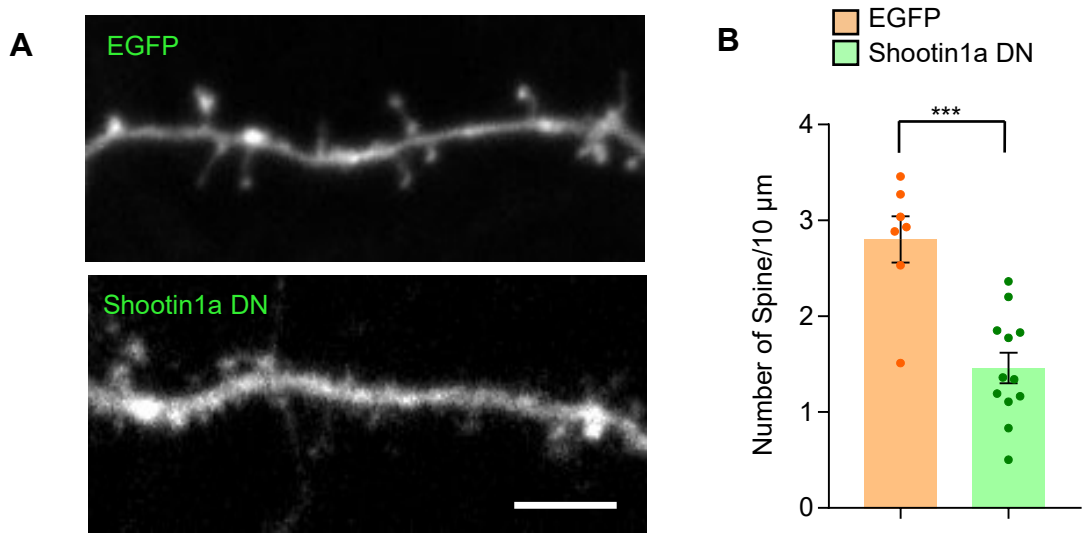

Figure 15. Disruption of shootin1a-mediated F-actin-adhesion clutch inhibits formation of dendritic spines. (A) DIV 14 primary hippocampal neurons were transfected with a control vector (pCAG-EGFP) or shootin1 dominant-negative (DN) (pCAG-GFP-shootin1 (1-125)) mutant. (B) Quantification of the protrusion number in control and DN-shootin1 neurons. Data represent n (control) = 7 neurons, n (shootin1 (1-125)) mutant = 12 neurons. Two-tailed unpaired Student's *t*-test ***p < 0.01. Scale Bar, 5 µm.

3.7 Shootin1a-mediated F-actin adhesion clutch is required for NMDA receptor-dependent spine plasticity

The formation of new spines, expansion of spine head, and shortening of spine neck have been observed under stimulation for long term potentiation (LTP) (Cornell-Bell et al., 1990; Bosch et al., 2014). Moreover, the spine head enlargement during LTP depends on the dynamics of actin filaments and is mediated by NMDA glutamate receptor activation (Krucker et al., 2000; Matsuzaki et al., 2001; Tanaka et al., 2008). Finally, I examined whether shootin1a-mediated clutch coupling plays a key role in synaptic plasticity. I used chemical LTP (cLTP) approach with glycine, a glutamate co-agonist, to induce structural plasticity (Hruska et al., 2018). Glycine induces LTP through the activation of NMDA receptors, which initiates by the entry of Ca^{2+} and that in turn triggers the activation of CaMKII (Lu et al., 2001).

The of NMDA receptor channels are blocked by Mg^{2+} ion, thereby preventing ions influx to flow through the cell membrane (Nowak et al., 1984; Zhu et al., 2016). Therefore, the induction of LTP was performed by addition of glycine in Mg^{2+}-free solution in DIV 14 cultured hippocampal neurons. Live imaging of neurons expressing GST or shootin1a-DN using confocal microscope was performed to monitor the changes in spine size. The addition of glycine induced the spine enlargement in DIV 14 neurons expressing GST (Figure 17). As reported previously (Hruska et al., 2018), addition of glycine induced sustained enlargement of 42% of dendritic spines. The spine enlargement was blocked by addition of AP5 and MK-801, indicating that the spine enlargement depends on NMDA receptor activation. Importantly, I found that disruption of shootin1a-mediated F-actin-adhesion coupling by shootin1-DN inhibited this NMDA receptor-dependent spine enlargement (Figure 17). Taken together, these data indicate that F-actin-clutch adhesion mediated by shootin1a plays an essential role in NMDA receptor-dependent spine plasticity.

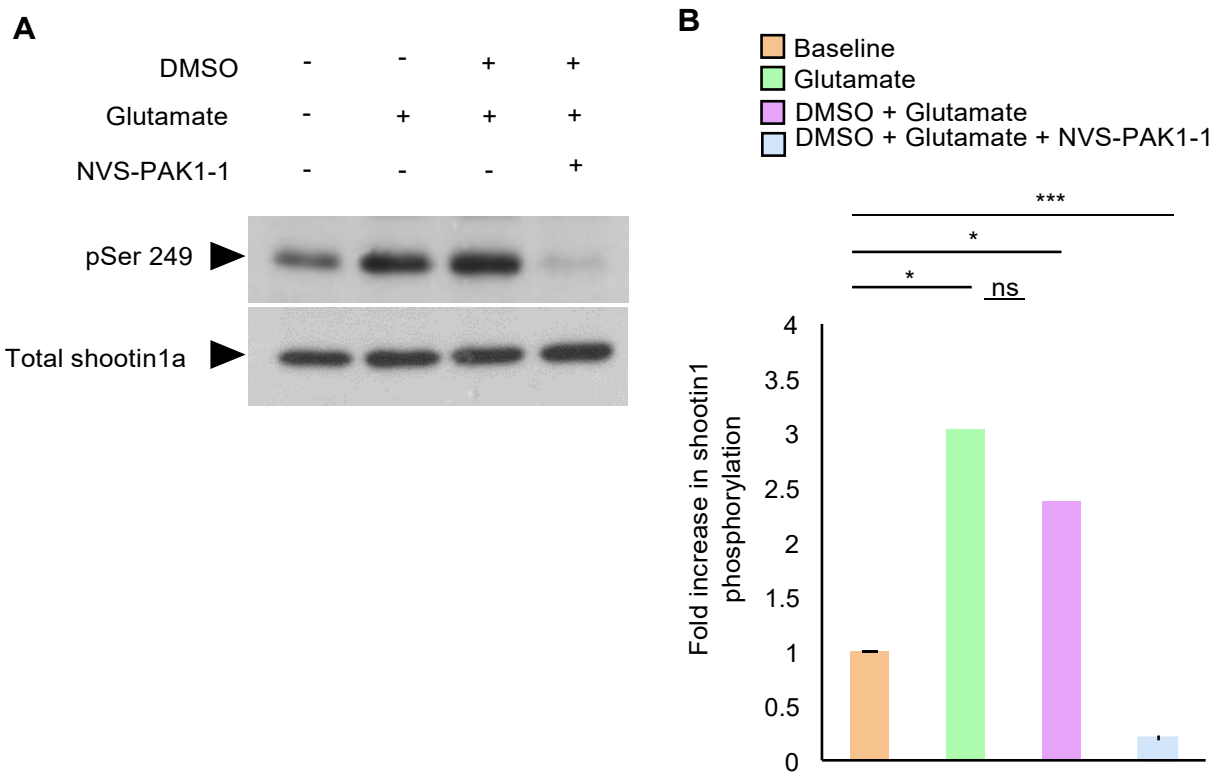

Figure 16. Glutamate stimulation induces PAK1-mediated shootin1a phosphorylation. (A) DIV 14 hippocampal neurons were treated without or with 10 μM glutamate (control). To inhibit Pak1 kinase upon glutamate stimulation, 10 μM glutamate was applied to DIV 14 neurons after 30 min incubation with 0.25 μM Inhibitor PAK-1 (NVS-PAK1-1). Cell lysate were then examined with immunoblotting with anti-pSer249 and anti-shootin1a antibodies. (B) Quantitative analysis of pSer249 after treated with 10 μM glutamate for 60 min and 0.25 μM Inhibitor PAK-1 (NVS-PAK1-1). Data represent means ± SEM; ***$p < 0.01$; **$p < 0.02$; *$p < 0.05$; ns, non significant.

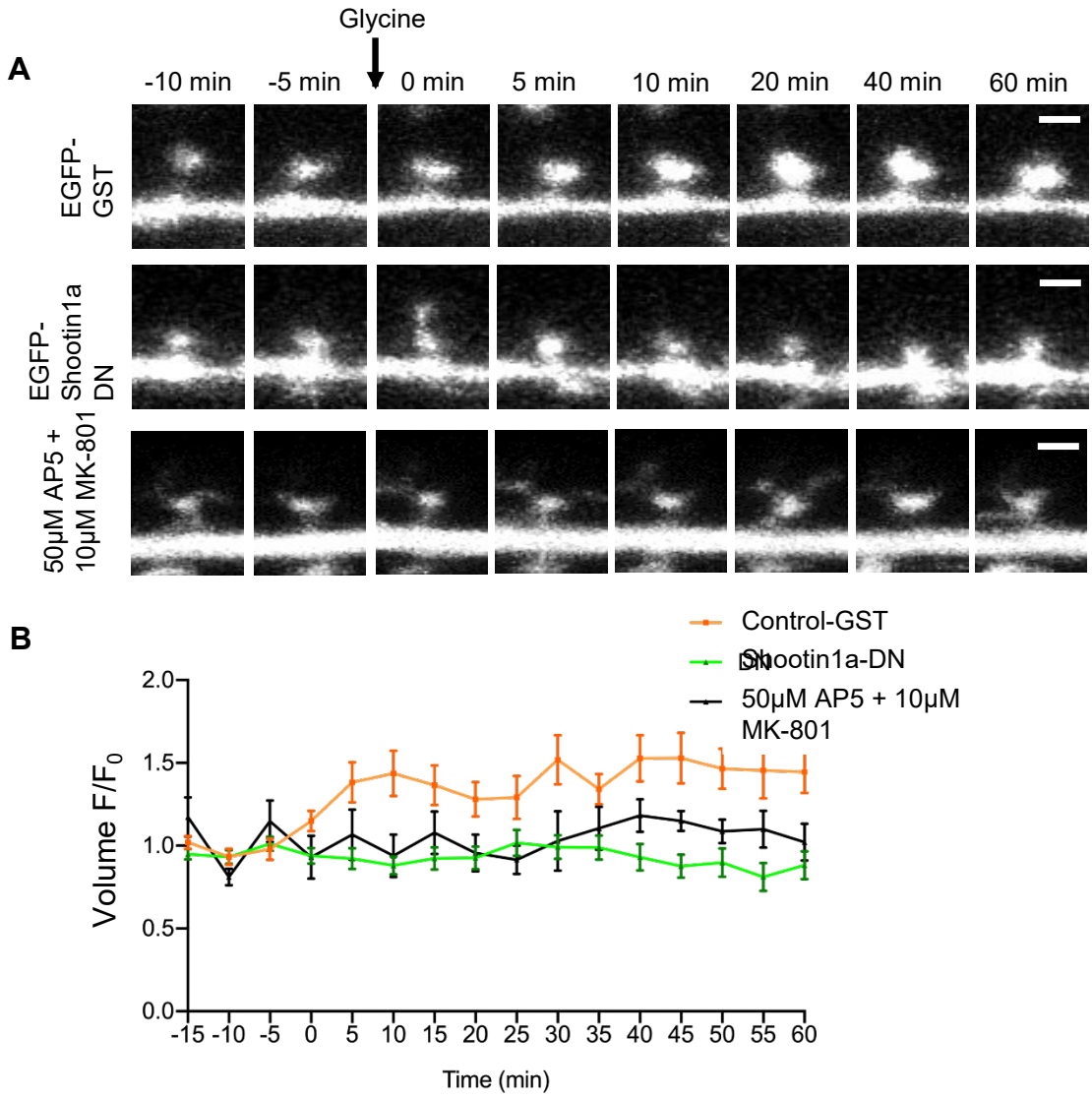

Figure 17. Disruption of shootin1a-mediated F-actin-adhesion clutch inhibits NMDR-dependent spine enlargement. (A) Representative images of time lapse of DIV 14 hippocampal neurons transfected with EGFP-GST and EGFP-shootin1a (1-125) before and after chemical LTP (cLTP). LTP were induced by glycine at 4 min before acquisition. Spine enlargement was blocked by treatment with 50μM AP5 and 10μM MK-801. (B) Increase in volume of dendritic spines before and after cLTP. Control-GST (orange line), n = 11 spines; EGFP-shootin1a (green line) (1-125), n = 14 spines; 50μM AP5 + 10μM MK-801 (black line), n = 6 spines. Bars, 1 μm.

4. Discussion

Shootin1a is reported to be expressed in early stages of developmental hippocampal neurons. Shootin1a functions as a clutch molecule in axonal growth cones (Toriyama et al., 2006; Kubo et al., 2015; Baba et al., 2018). Here, I found that shootin1a is also expressed at later stages of cultured hippocampal neurons and localized in dendritic spines. Shootin1a mediated F-actin-adhesion clutch generates traction force on adhesion substrate for the formation and maturation of dendritic spines. Furthermore, shootin1a-mediated F-actin-adhesion clutch is necessary for NMDA receptor-dependent spine enlargement. This study demonstrates that mechanical regulation of F-actin-adhesion coupling mediated by shootin1a is necessary for the formation and plasticity of dendritic spines.

4.1 Shootin1a is required for the formation and maturation of dendritic spines

In this study, I showed that shootin1a is localized at the tip of filopodia-like and stubby spines. Filopodia-like spines are the precursors of dendritic spines (Ziv and Smith, 1996). On the other hand, stubby spine is proposed (by the Miller/Peters Model (1981)) as an early stage in the process of spine protrusion which in turn to form mushroom-shaped spines. Thus, here I hypothesized that shootin1a may play a role in spine formation. The formation of spines is thought to be originated from patches of actin filament on dendritic shafts and it has network-like cytoskeleton organization without any bundling protein (Korobova and Svitkina, 2010). A number of actin regulatory proteins have been known to play important roles in regulating the actin dynamic during spine formation. The Arp2/3 complex is the most well-known protein in the process of actin filaments elongation (Hotulainen and Hoogenraad, 2010). The Arp2/3 complex produces a dense branched of actin network to expand of spine head (Korobova and Svitkina, 2010; Chazeau et al., 2014). The mDia2/formin protein is required for proper spine formation by promoting the polymerization of actin filament at tip of filopodia-like spines (Hotulainen et al., 2009). Moreover, It has been shown that neuronal activity regulates the initiation of dendritic filopodia but not in the growth cone (Portera-Cailliau et al., 2003). The present study demonstrated that overexpression and loss of shootin1a resulted in an increase and reduction the number of PSD-95-positive puncta, respectively, suggesting that shootin1a is required for spine formation.

PSD-95, a best-known scaffolding protein in dendritic spines, binds with NMDA receptors and stabilizes dendritic spine plasticity (Chen et al., 2011; Zhu et al., 2016a; Won et al., 2016). PSD-95 is partially anchored by F-actin at the spines from 13 days culture of

neurons (Zhang and Benson, 2001). The transition of filopodia-like spines into mature spines is regulated by several regulators of actin polymerization such as Arp2/3, cortactin, myosin II, cofilin and profilin (Fukazawa et al., 2003; Ackermann and Matus, 2003; Gu et al., 2010; Hodges et al., 2011; Catarino et al., 2013; Spence et al., 2016). Interestingly, I found that shootin1-KO mice brain exhibits a decreased number of mushroom-shaped spines and an increment number of filopodia-like spines. Therefore, these results suggest that shootin1a is involved in the maturation of dendritic spines.

4.2 Shootin1a mediates F-actin-adhesion clutch for dendritic spine formation

The polymerization and de-polymerization of actin cytoskeleton plays a pivotal role in both structure and dynamic of dendritic spines. The growth of new actin network at the leading edge is considered to be essential for pushing the cell membrane forward (Ananthakrishnan and Ehrlicher, 2007). Myosin II activity in filopodia spines induces retrograde flow of F-actin (Portera-Cailliau et al., 2003; Medeiros et al., 2006; Korobova and Svitkina, 2010). In dendritic spines, retrograde flow of F-actin was observed in filopodia-like and at the edge of expanding spine head (Honkura et al., 2008; Tatavarty et al., 2009, 2012). Consistently in this study, I found that F-actin flows retrogradely in filopodia-like spines (Figure 11).

Shootin1a is a clutch molecule that plays an important role in axon outgrowth and guidance (Toriyama et al., 2006, 2013; Kubo et al., 2015; Abe et al., 2018; Baba et al., 2018). Previously, it is reported that shootin1a-cortactin interaction couples retrograde flow of F-actin with extracellular substrate via L1-CAM in axonal growth cone (Kubo et al., 2015; Baba et al., 2018). Co-localization of shootin1a, cortactin, and L1-CAM in dendritic spines suggests that similar interactions may occur during morphogenesis of dendritic spines. Moreover, I found that shootin1a and cortactin speckles moved retrogradely in filopodia-like spines as well as F-actin speckles, suggesting that shootin1a may link F-actin retrograde flow with adhesive substrates. Several cell adhesion molecules (CAM) are reported to have important contributions in synapse formation and regulation of spine morphology, such as N-CAM and neuroligin 1. These regulations occur through signaling cascades or secondary protein-protein interactions (Dalva et al., 2007; Liu et al., 2016). In addition, it is reported that extracellular cell molecules accumulate at the edges of pre- and post-synaptic appositions of the neurons and astrocytes, including dendritic spines (Tian et al., 1997; Levy et al., 2014; Omar et al., 2017), suggesting that cell adhesion molecules may mediate physical interactions

with dendritic spine membrane to modulate synapse formation, maturation and synaptic plasticity.

The present study demonstrates that disruption shootin1-L1-CAM interaction increased F-actin retrograde flow in the filopodia-like spines (Figure 11), indicating that inhibition of shootin1a-mediated F-actin-adhesion clutch in dendritic spines. Importantly, the inhibition of shootin1a-mediated F-actin-adhesion clutch in spines also reduced significantly the generation of traction force in spines (Figure 14), which in turn resulted in reduction in a number of dendritic spines (Figure 15). Based on this notion, I consider that shootin1a mechanically couples F-actin retrograde flow and cell adhesion, through its interaction with cortactin and L1-CAM, thereby generating force for the formation dendritic spines.

4.3 Glutamate induces Pak1-mediated shootin1a phosphorylation in dendritic spines

Glutamate is one of the major of excitatory neurotransmitter in the mammalian nervous system. Activation of NMDA receptor by glutamate allows ion Na^+ and Ca^+ influx, thereby triggers a series of signaling pathway (Tanaka et al., 2008; Fortin et al., 2010). Calcium influx promotes the activation of a serine/threonine protein kinase, Ca^{2+}/Calmodulin-dependent protein kinase II (CaMKII) in dendritic spines (Inagaki et al., 2000; Okamoto et al., 2007; Redondo and Morris, 2011; Bosch et al., 2014). This in turn stimulates the activation of cdc42 and Rac1, and βpix (Asrar et al., 2009; Bosch et al., 2014; Shin et al., 2019). In response to glutamate uncaging stimulation, spines can undergo structural plasticity by enlarging their size (Matsuzaki et al., 2001; Murakoshi et al., 2011; Bosch et al., 2014). Interestingly, my study showed that glutamate induces Pak1-mediated shootin1a phosphorylation at Ser249 (Figure 16). Our previous study showed that Pak1-mediated shootin1a phosphorylation at Ser101 and Ser249 enhances the coupling between F-actin retrograde flow and L1-CAM at growth cone (Toriyama et al., 2013). Together, these results suggest that glutamate-induced phosphorylation of shootin1a may enhance the F-actin adhesion clutch to enlarge the head of dendritic spines.

The proposed signaling pathway of shootin1a-mediated F-actin-adhesion clutch coupling for the generation of traction force in spine expansion is described in Figure 18. Induction of actin polymerization and signal-force conversion of F-actin may work coordinately to efectively regulate the formation and expansion of dendritic spines under glutamate stimulation.

4.4 Shootin1a-L1-CAM interaction mediates NMDA receptor-dependent spine plasticity

During LTP, actin filaments undergo dynamic rearrangement, which in turn induces structural expansion of dendritic spine head (sLTP). Regulatory proteins that is involved in activity-induced spine enlargement have been extensively studied. Spine enlargement is associated with an increase in AMPA-receptor-mediated current and is dependent on NMDA receptors, calmodulin and actin polymerization (Krucker et al., 2000; Matsuzaki et al., 2001). In addition, it is reported that the speed of actin flow is faster in large spine than in small spines, suggesting a higher rate of actin polymerization in larger spines (Honkura et al., 2008). The present study indicates that inhibition of shootin1a-mediated F-actin-adhesion clutch coupling by dominant-negative of shootin1a also inhibits the spine enlargement after LTP induction. This finding suggest that the coupling of F-actin flow and adhesive substrate regulates the expansion of spines.

The dynamic nanoscale of F-actin nucleation and elongation determines the shape of dendritic spines. Nucleation of F-actin networks occurs close to PSD, while elongations of F-actin barbed end (+) is located at the tips of protrusion emerging from the spine head (Spacek, 2004; Chazeau et al., 2014). In addition, plasticity of dendritic spines is dynamically and mechanically regulated by dynamic, stable and enlargement pool of F-actin (Honkura et al., 2008). Therefore, it is speculated that the spine enlargement of dendritic spine must be induced by mechanical force generated by F-actin pool in spines. Although, this present study did not demonstrate the generation traction force in mature spines, the involvement of shootin1a in spine enlargement could explains that the mechanical clutch is required to produce force during synaptic plasticity.

Moreover, activity-dependent modification or degradation of extracellular matrix (ECM) proteins affects the growth and morphology of dendritic spines (Dityatev et al., 2010). Laminin was first identified as an important molecule in developing synapse structure and function at the neuromuscular junction (NMJ). Mice lacking laminin α4 or β2 have misaligned NMJs and altered synaptic functions (Noakes et al., 1995; Patton et al., 2001). Laminin provides structural support to neuron by incorporating into insoluble matrix surrounding. It was found that laminin interacts with L1-CAM and increased the generation of traction force of axonal growth cone (Abe et al., 2018). This notion raises the possibility that L1-CAM and laminin may interact and regulate the F-actin-adhesion clutch in dendritic spines.

The abnormality in spine morphology is associated with neurological disorders and alteration in actin cytoskeleton. Neurons from individual with intellectual disability have a low number of dendritic spines with immature morphology (Forrest et al., 2018). Mutation in transcription factor, CCNT2, in intellectual disability patients leads to the down-regulation of genes that is related with actin cytoskeleton, axonogenesis and protein kinase. And, recent study reported that shootin1 gene is one of the most significantly down-regulated genes in the patients (InanlooRahatloo et al., 2019). The present findings about the role of shootin1a in dendritic spine will enhance our understanding of the molecular mechanics that underlie the spine abnormality in neurological disorders.

4.5 Conclusion

The present work demonstrated that shootin1a is expressed in the later developmental stages and is localized in dendritic spines. Figure 18 shows a proposed model of molecular mechanics mediated by shootin1a of spine formation, maturation and plasticity (Figure 19A, dashed line box). Shootin1a-L1-CAM interaction mediates the physical linkage between F-actin retrograde flow and extracellular substrate. This mechanical machinery generates the traction force against the substrate, which helps in the formation and plasticity of dendritic spines (Figure 19B). A recent study reports that whole-transcriptome analysis from blood samples of intellectual disability patients showed a down-regulation of shootin1 gene (InanlooRahatloo et al., 2019). I hope the present roles of shootin1a in spine formation and synaptic plasticity provide a better understanding mechanobiological mechanism in neurological disorders.

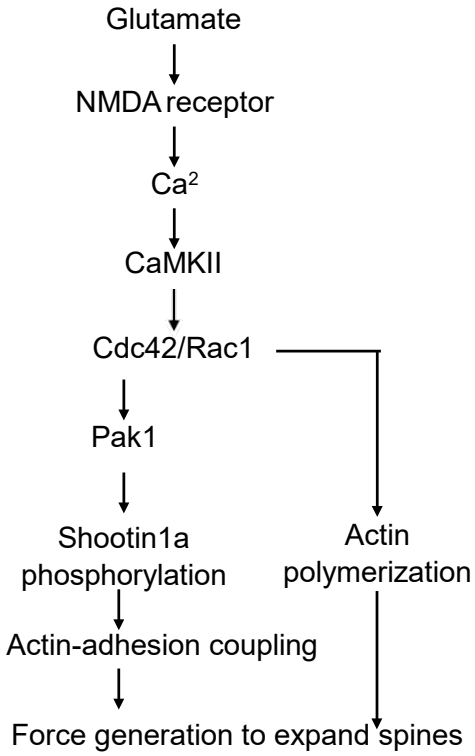

Figure 18. A proposed signaling pathway shootin1a-mediated F-actin-adhesion clutch coupling for the generation of traction force in spine formation and synaptic plasticity

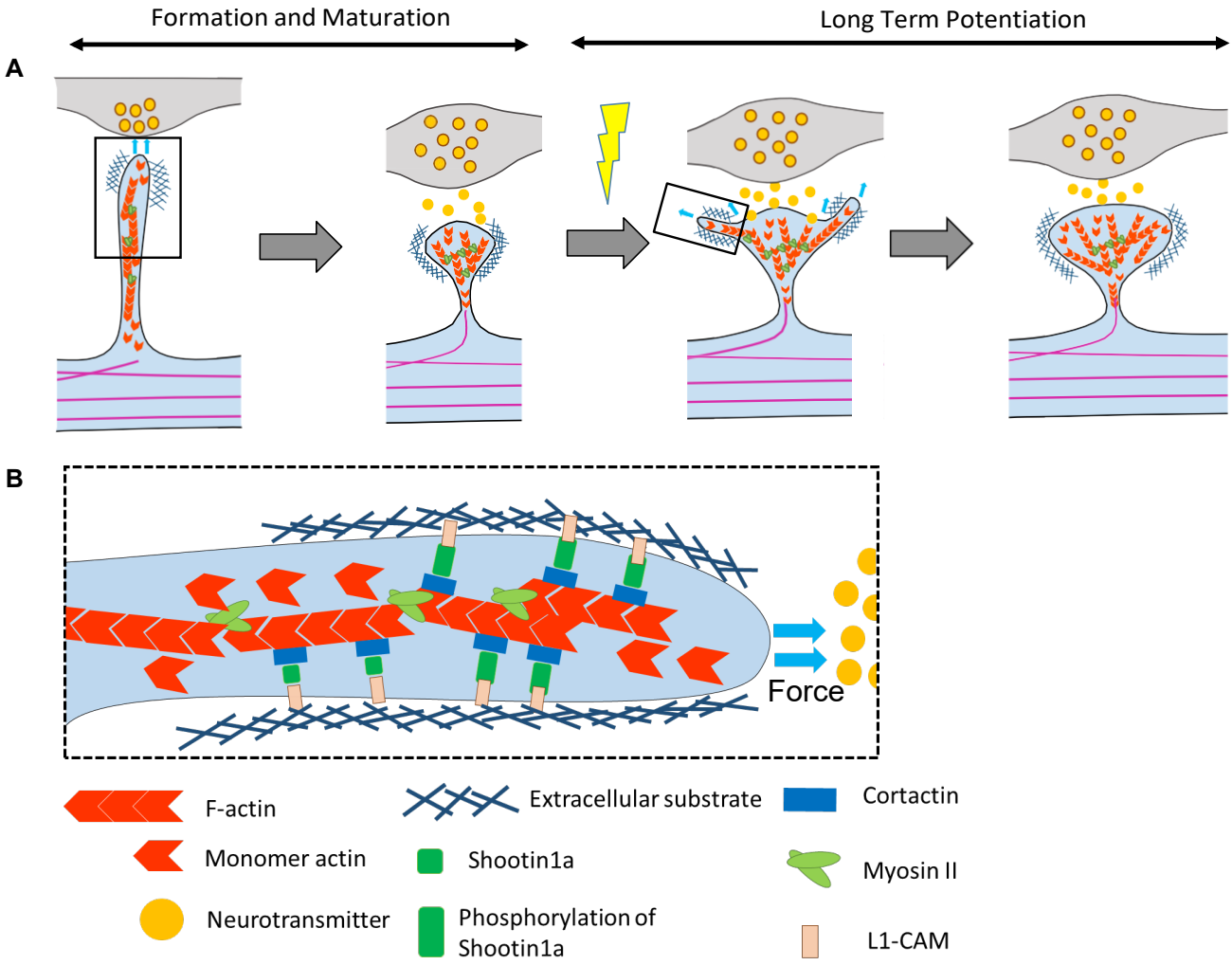

Figure 19. (A) A proposed model of molecular clutch mechanism in the dendritic spine formation and synaptic plasticity (dashed box). The traction force is generated by F-actin-adhesion coupling in the filopodia-like spines and in the head expansion of mature spine (blue arrows). (B) Shootin1a-L1-CAM interaction mediates the physical linkage between F-actin retrograde flow and extracellular substrates. This mechanical machinery generates the traction force against the substrate, which helps in the spine formation and synaptic plasticity.

Acknowledgements

Alhamdulillah. I praise and thank to ALLAH SWT for His greatness and for giving me the strength and courage to complete this thesis.

First and foremost, I owe this extraordinary opportunity for the last five years of my life to my advisor Professor Naoyuki Inagaki. His guidance and kindness will never cease to inspire me to be a better thinker and better person, particularly in science field. Next, I want to recognize my committee member Professor Shiro Suetsugu and Associate Professor Noriaki Sasai for their perceptive suggestions and valuable comments.

Next, I want to give my special thank for our former postdoc fellows in our lab, Dr. Hiroko Katsuno, who teached me and always support me in the beginning of my life in Japan, either as scientist or as a friend. As a woman, she is a nice mentor and I have much to learn from her intrepid attitude in both science and life. In addition, I thank to Assistant Professor Kentarou Baba and a Postdoc fellow Takunori Minegishi for helping my project and reviewing my doctoral thesis.

My acknowledgement also goes to our secretary, Mieko Ueda, for helping me a lot in every difficulty of my daily life in the Lab.

I also would like to thank the international students in the Lab, Saranpal Singh Satinder Singh and Kaewkascholkul Napol, who mentally support and help me for many things happen during my study in the NAIST. Many thanks for all my lab fellows for their technical assistance and helpful suggestion.

I am in debt to my family for their endless love, care, and support throughout my entire life. Especially to my mother, who always send her love and pray for my success, luck and my healthy. I also dedicate all my work for my late father.

I would like to acknowledge all Indonesian student families in NAIST for making me feel that I am not alone in NAIST.

I would like to extend my thanks to MEXT: Ministry of Education, Culture, Sport, Science and Technology Japan for their financial support during my study in NAIST.

Reference

Abe, K., H. Katsuno, M. Toriyama, K. Baba, T. Mori, T. Hakoshima, Y. Kanemura, R. Watanabe, and N. Inagaki. 2018. Grip and slip of L1-CAM on adhesive substrates direct growth cone haptotaxis. *Proc. Natl. Acad. Sci.* USA 115:2764–2769.

Ackermann, M., and A. Matus. 2003. Activity-induced targeting of profilin and stabilization of dendritic spine morphology. *Nat. Neurosci.* 6:1194–1200.

Ananthakrishnan, R., and A. Ehrlicher. 2007. The forces behind cell movement. *Int J Biol Sci*. 3:303–317.

Asrar, S., Y. Meng, Z. Zhou, Z. Todorovski, W.W. Huang, and Z. Jia. 2009. Regulation of hippocampal long-term potentiation by p21-activated protein kinase 1 (PAK1). *Neuropharmacology*. 56:73–80.

Baba, K., W. Yoshida, M. Toriyama, and T. Shimada. 2018. Gradient-reading and mechano-effector machinery for netrin-1-induced axon guidance. *Elife*. 7:1–35.

Basu, S., and R. Lamprecht. 2018. The Role of Actin Cytoskeleton in Dendritic Spines in the Maintenance of Long-Term Memory. *Front. Mol. Neurosci.* 11:1–9.

Bear, M.F., and R.C. Malenka. 1991. Synaptic plasticity: LTP and LTD. *Curr. Opin. Neurobiol.* 1:113–20.

Borczyk, M., M.A. Śliwińska, A. Caly, T. Bernas, and K. Radwanska. 2019. Neuronal plasticity affects correlation between the size of dendritic spine and its postsynaptic density. *Sci. Rep.* 9:1–12.

Bosch, M., J. Castro, T. Saneyoshi, H. Matsuno, M. Sur, and Y. Hayashi. 2014. Structural and molecular remodeling of dendritic spine substructures during long-term potentiation. *Neuron*. 82:2166–2171.

Catarino, T., L. Ribeiro, S.D. Santos, and A.L. Carvalho. 2013. Regulation of synapse composition by protein acetylation: the role of acetylated cortactin. *J. Cell Sci.* 126:149–162.

Chazeau, A., A. Mehidi, D. Nair, J.J. Gautier, C. Leduc, I. Chamma, F. Kage, A. Kechkar, O. Thoumine, K. Rottner, D. Choquet, A. Gautreau, J. Sibarita, and G. Giannone. 2014. Nanoscale segregation of actin nucleation and elongation factors determines dendritic spine protrusion. *EMBO J.* 33:2745–2764.

Chen, X., C.D. Nelson, X. Li, C.A. Winters, R. Azzam, A.A. Sousa, R.D. Leapman, H. Gainer, M. Sheng, and T.S. Reese. 2011. PSD-95 is required to sustain the molecular organization of the postsynaptic density. *J. Neurosci.* 31:6329–6338.

.

Cornell-Bell, A.H., P.G. Thomas, and S.J. Smith. 1990. The excitatory neurotransmitter glutamate causes filopodia formation in cultured hippocampal astrocytes. *Glia*. 3:322–334.

Cruz-Martin, A., M. Crespo, and C. Portera-Cailliau. 2010. Delayed stabilization of dendritic spines in fragile X mice. *J. Neurosci.* 30:7793–7803.

Cruz-Martín, A., M. Crespo, and C. Portera-Cailliau. 2012. Glutamate induces the elongation of early dendritic protrusions via mGluRs in wild type mice, but not in fragile X mice. *PLoS One*. 7:1–9.

Dalva, M.B., A.C. McClelland, and M.S. Kayser. 2007. Cell adhesion molecules: Signalling functions at the synapse. *Nat. Rev. Neurosci.* 8:206–220.

DeFelipe, J. 2006. Brain plasticity and mental processes: Cajal again. *Nat. Rev. Neurosci.* 7:811–817.

Dityatev A., M. Schachner, P. Sonderegger . 2010. The dual role of the extracellular matrix in synaptic plasticity and homeostasis. *Nature Rev. Neurosci*. 11:735-46.

Fan, Y., X. Tang, E. Vitriol, G. Chen, and J.Q. Zheng. 2011. Actin capping protein is required for dendritic spine development and synapse formation. *J. Neurosci.* 31:10228–10233.

Forrest, M.P., E. Parnell, and P. Penzes. 2018. Dendritic structural plasticity and neuropsychiatric disease. *Nat. Rev. Neurosci.* 19:215–234.

Fortin, D.A., M.A. Davare, T. Srivastava, J.D. Brady, S. Nygaard, V.A. Derkach, and T.R. Soderling. 2010. Long-term potentiation-dependent spine enlargement requires synaptic Ca^{2+}-permeable AMPA receptors recruited by CaM-Kinase I. *J. Neurosci.* 30:11565–11575.

Frankfurt, M., and V. Luine. 2015. The evolving role of dendritic spines and memory: Interaction(s) with estradiol. *Horm. Behav.* 74:28–36.

Fukazawa, Y., Y. Saitoh, F. Ozawa, Y. Ohta, K. Mizuno, and K. Inokuchi. 2003. Hippocampal LTP is accompanied by enhanced F-actin content within the dendritic spine that is essential for late LTP maintenance in vivo. *Neuron*. 38:447–460.

Gu, J., C.W. Lee, Y. Fan, D. Komlos, X. Tang, C. Sun, K. Yu, H.C. Hartzell, G. Chen, J.R. Bamburg, and J.Q. Zheng. 2010. ADF/cofilin-mediated actin dynamics regulate AMPA receptor trafficking during synaptic plasticity. *Nat. Neurosci.* 13:1208–1215.

Hammond, C., J.-M. Goaillard, D. Debanne, and J.-L. Gaiarsa. 2015. Synaptic plasticity. Fourth Edi. Academic Press. p361-389 pp.

Harris, K.M., F.E. Jensen, and B. Tsao. 1992. Three-dimensional structure of dendritic spines and synapses in rat hippocampus (CA1) at postnatal day 15 and adult ages: Implication for the maturation of synaptic physiology and long term potentiation. *J. Neurosci.* 12:2685–2705.

Hayashi, K., T. Oshima, M. Hashimoto, and K. Mikoshiba. 2007. Pak1 regulates dendritic branching and spine formation. *Dev. Neurobiol.* 655–669.

Hayashi, M.L., S.Y. Choi, B.S. Shankaranarayana Rao, H.Y. Jung, H.K. Lee, D. Zhang, S. Chattarji, A. Kirkwood, and S. Tonegawa. 2004. Altered cortical synaptic morphology and impaired memory consolidation in forebrain- specific dominant-negative PAK transgenic mice. *Neuron*. 42:773–787.

Hering, H., and M. Sheng. 2001. Dendritic spines: structure, dynamics and regulation. *Nat. Rev. Neurosci.* 2:880–888.

Hering, H., and M. Sheng. 2003. Activity-dependent redistribution and essential role of cortactin in dendritic spine morphogenesis. *J Neurosci*. 23:11759–11769.

Herms, J., and M.M. Dorostkar. 2016. Dendritic Spine Pathology in Neurodegenerative Diseases. *Annu. Rev. Pathol. Mech. Dis.* 11:221–250.

Higashiguchi, Y., K. Katsuta, T. Minegishi, S. Yonemura, A. Urasaki, and N. Inagaki. 2016. Identification of a shootin1 isoform expressed in peripheral tissues. *Cell Tissue Res.* 366:75–87.

Hodges, J.L., K. Newell-Litwa, H. Asmussen, M. Vicente-Manzanares, and A.R. Horwitz. 2011. Myosin IIB activity and phosphorylation status determines dendritic spine and post-synaptic density morphology. *PLoS One*. 6:e24149.

Honkura, N., M. Matsuzaki, J. Noguchi, G.C.R. Ellis-Davies, and H. Kasai. 2008. The Subspine organization of actin fibers regulates the structure and plasticity of dendritic spines. *Neuron*. 57:719–729.

Hotulainen, P., and C.C. Hoogenraad. 2010. Actin in dendritic spines: Connecting dynamics to function. *J. Cell Biol.* 189:619–629.

Hotulainen, P., O. Llano, S. Smirnov, K. Tanhuanpää, J. Faix, C. Rivera, and P. Lappalainen. 2009. Defining mechanisms of actin polymerization and depolymerization during dendritic spine morphogenesis. *J. Cell Biol.* 185:323–339.

Hruska, M., N. Henderson, S.J. Le Marchand, H. Jafri, and M.B. Dalva. 2018. Synaptic nanomodules underlie the organization and plasticity of spine synapses. *Nat. Neurosci.* 21:671–682.

Inagaki, N., M. Nishizawa, N. Arimura, H. Yamamoto, Y. Takeuchi, E. Miyamoto, K. Kaibuchi, and M. Inagaki. 2000. Activation of $Ca^{2+/}$calmodulin-dependent protein kinase II within post-synaptic dendritic spines of cultured hippocampal neurons. *J. Biol. Chem.* 275:27165–27171.

InanlooRahatloo, K., F. Peymani, K. Kahrizi, and H. Najmabadi. 2019. Whole-transcriptome analysis reveals dysregulation of actin-cytoskeleton pathway in intellectual disability patients. *Neuroscience*. 404:423–444.

Kaech, S., and G. Banker. 2006. Culturing hippocampal neurons. *Nat. Protoc.* 1:2406–2415.

Karpov, A.S., P. Amiri, C. Bellamacina, M.H. Bellance, W. Breitenstein, D. Daniel, R. Denay, D. Fabbro, C. Fernandez, I. Galuba, S. Guerro-Lagasse, S. Gutmann, L. Hinh, W. Jahnke, J. Klopp, A. Lai, M.K. Lindvall, S. Ma, H. Möbitz, S. Pecchi, G. Rummel, K. Shoemaker, J. Trappe, C. Voliva, S.W. Cowan-Jacob, and A.L. Marzinzik. 2015. Optimization of a Dibenzodiazepine Hit to a Potent and Selective Allosteric PAK1 Inhibitor. *ACS Med. Chem. Lett.* 6:776–781.

Katsuno, H., M. Toriyama, Y. Hosokawa, K. Mizuno, K. Ikeda, Y. Sakumura, and N. Inagaki. 2015. Actin migration driven by directional assembly and disassembly of membrane-anchored actin filaments. *Cell Rep.* 12:648–660.

Koganezawa, N., K. Hanamura, Y. Sekino, and T. Shirao. 2016. The role of drebrin in dendritic spines. *Mol. Cell. Neurosci.* 84:85–92.

Korobova, F., and T. Svitkina. 2010. Molecular architecture of synaptic actin cytoskeleton in hippocampal neurons reveals a mechanism of dendritic spine morphogenesis. *Mol. Biol. Cell*. 21:165–176.

Krucker, T., G.R. Siggins, and S. Halpain. 2000. Dynamic actin filaments are required for stable long-term potentiation (LTP) in area CA1 of the hippocampus. *Proc. Natl. Acad. Sci.* 97:6856–6861.

Kubo, Y., K. Baba, M. Toriyama, T. Minegishi, T. Sugiura, S. Kozawa, K. Ikeda, and N. Inagaki. 2015. Shootin1-cortactin interaction mediates signal-force transduction for axon outgrowth. *J. Cell Biol.* 210:663–676.

Lei, W., O.F. Omotade, K.R. Myers, and J.Q. Zheng. 2016. Actin Cytoskeleton in Dendritic Spine Development and Plasticity. *Curr. Opin. Neurobiol.* 39:86–92.

Levy, A.D., M.H. Omar, and A.J. Koleske. 2014. Extracellular matrix control of dendritic spine and synapse structure and plasticity in adulthood. *Front. Neuroanat.* 8:1–18.

Lisman, J., R. Yasuda, and S. Raghavachari. 2012. Mechanisms of CaMKII action in long-term potentiation. *Nat. Rev. Neurosci.* 13:169–182.

Liu, A., Z. Zhou, R. Dang, Y. Zhu, J. Qi, G. He, C. Leung, D. Pak, Z. Jia, and W. Xie. 2016. Neuroligin 1 regulates spines and synaptic plasticity via LIMK1/cofilin-mediated actin reorganization. *J. Cell Biol.* 212:449–463.

Llinás, R.R. 2003. The contribution of Santiago Ramon y Cajal to functional neuroscience. *Nat. Rev. Neurosci.* 4:77–80.

Los, G. V, L.P. Encell, M.G. Mcdougall, D.D. Hartzell, N. Karassina, D. Simpson, J. Mendez, K. Zimmerman, P. Otto, G. Vidugiris, and J. Zhu. 2008. HaloTag: A novel protein labeling technology for cell imaging and protein analysis. *ACS Chem. Biol.* 3:373–382.

Lu, W.-Y., H.-Y. Man, W. Ju, W.S. Trimble, J.F. MacDonald, and Y.T. Wang. 2001. Activation of synaptic NMDA receptors induces membrane insertion of new AMPA receptors and LTP in cultured hippocampal neurons. *Neuron*. 29:243–254.

Malenka, R.C., and M.F. Bear. 2004. LTP and LTD: Review an embarrassment of riches. *Neuron*. 44:5–21.

Mateos-Aparicio, P., and A. Rodríguez-Moreno. 2019. The impact of studying brain plasticity. *Front. Cell. Neurosci.* 13:1–5.

Matsuzaki, M., N. Honkura, G.C.R. Ellis-Davies, and H. Kasai. 2001. Structural basis of long-term potentiation in single dendritic spines. *Nature*. 429:761–766.

Medeiros, N.A., D.T. Burnette, and P. Forscher. 2006. Myosin II functions in actin-bundle turnover in neuronal growth cones. *Nat. Cell Biol.* 8:215–226.

Minegishi, T., Y. Uesugi, N. Kaneko, W. Yoshida, K. Sawamoto, and N. Inagaki. 2018. Shootin1b mediates a mechanical clutch to produce force for neuronal migration. *Cell Rep.* 25:624-639.e6.

Moyer, C.E., M.A. Shelton, and R.A. Sweet. 2015. Dendritic spine alterations in schizophrenia. *Neurosci. Lett.* 601:46–53.

Murakoshi, H., H. Wang, and R. Yasuda. 2011. Local, persistent activation of Rho GTPases during plasticity of single dendritic spines. *Nature*. 472:100–104.

Newey, S.E., V. Velamoor, E.E. Govek, and L. Van Aelst. 2005. Rho GTPases, dendritic structure, and mental retardation. *J. Neurobiol.* 64:58–74.

Nimchinsky, E.A., B.L. Sabatini, and K. Svoboda. 2002. Structure and Function of Dendritic Spines. *Annu. Rev. Physiol.* 64:313–353.

Noakes, P.G., M. Gautam, J. Mudd, J. R. Sanes and J.P. Merlie. 1995 Aberrant differentiation of neuromuscular junctions in mice lacking s-laminin/laminin beta 2. *Nature*. 374:258-62.

Nowak, L., P. Bregestovski, P. Ascher, A. Herbet, and A. Prochiantz. 1984. Magnesium gates glutamate-activated channels in mouse central neurones. *Nature*. 307:462–465.

Okamoto, K.-I., R. Narayanan, S.H. Lee, K. Murata, and Y. Hayashi. 2007. The role of CaMKII as an F-actin-bundling protein crucial for maintenance of dendritic spine structure. *Proc. Natl. Acad. Sci.* 104:6418–6423.

Omar, M.H., M.K. Campbell, X. Xiao, Q. Zhong, W.J. Brunken, J.H. Miner, C.A. Greer, and A.J. Koleske. 2017. CNS neurons deposit laminin α5 to stabilize synapses. *Cell Rep.* 21:1281–1292.

Patton B.L., J.M. Cunningham, J. Thyboll, J. Kortesmaa, H. Westerblad, L. Edstrom. 2001. Property formed but improperly localized synaptic specializations in the absence of laminin alpha4. *Nature Neurosci*. 4:597-604.

Penzes, P., M.E. Cahill, K.A. Jones, J.E. Vanleeuwen, and K.M. Woolfrey. 2011. Dendritic spine pathology in neuropsychiatric disorders. *Nat. Neurosci.* 14:285–293.

Portera-Cailliau, C., D.T. Pan, and R. Yuste. 2003. Activity-regulated dynamic behavior of early dendritic protrusions: evidence for different types of dendritic filopodia. *J. Neurosci. Off. J. Soc. Neurosci.* 23:7129–7142.

Racaniello, M., A. Cardinale, C. Mollinari, M. D'Antuono, G. De Chiara, V. Tancredi, and D. Merlo. 2010. Phosphorylation Changes of CaMKII, ERK1/2, PKB/Akt Kinases and CREB Activation during Early Long-Term Potentiation at Schaffer Collateral-CA1 Mouse Hippocampal Synapses. *Neurochem. Res.* 35:239–246.

Redondo, R.L., and R.G.M. Morris. 2011. Making memories last: The synaptic tagging and capture hypothesis. *Nat. Rev. Neurosci.* 12:17–30.

Risher, W.C., T. Ustunkaya, J.S. Alvarado, and C. Eroglu. 2014. Rapid golgi analysis method for efficient and unbiased classification of dendritic spines. *PLoS One*. 9:e107591.

Semenova, G., and J. Chernoff. 2017. Targeting PAK1. *Biochem. Soc. Trans.* 45:79–88.

Sheng, M., and C.C. Hoogenraad. 2007. The Postsynaptic Architecture of Excitatory Synapses: A More Quantitative View. *Annu. Rev. Biochem.* 76:823–847.

Shimada, T., M. Toriyama, K. Uemura, H. Kamiguchi, T. Sugiura, N. Watanabe, and N. Inagaki. 2008. Shootin1 interacts with actin retrograde flow and L1-CAM to promote axon outgrowth. *J. Cell Biol.* 181:817–829.

Shin, M., S. Song, J.E. Shin, S.-H. Lee, S.-O. Huh, and D. Park. 2019. Src-mediated phosphorylation of βPix-b regulates dendritic spine morphogenesis. *J. Cell Sci.*

Sotelo, C. 2003. Viewing the brain through the master hand of Ramon y Cajal. *Nat. Rev. Neurosci.* 4:71–77.

Spacek, J. 2004. Trans-endocytosis via spinules in adult rat hippocampus. *J. Neurosci.* 24:4233–4241.

Spence, E.F., D.J. Kanak, B.R. Carlson, and S.H. Soderling. 2016. The Arp2/3 complex is essential for distinct stages of spine synapse maturation, including synapse unsilencing. *J. Neurosci.* 36:9696–9709.

Tada, T., and M. Sheng. 2006. Molecular mechanisms of dendritic spine morphogenesis. *Curr. Opin. Neurobiol.* 16:95–101.

Tanaka, J., Y. Horiike, M. Matsuzaki, T. Miyazaki, G.C.R. Ellis-Davies, and H. Kasai. 2008. Protein synthesis and neurotrophin-dependent structural plasticity of single dendritic spines. *Science.* 319:1683–1687.

Tatavarty, V., S. Das, and J. Yu. 2012. Polarization of actin cytoskeleton is reduced in dendritic protrusions during early spine development in hippocampal neuron. *Mol. Biol. Cell*. 23:3167–3177.

Tatavarty, V., E.J. Kim, V. Rodionov, and J. Yu. 2009. Investigating sub-spine actin dynamics in rat hippocampal neurons with super-resolution optical imaging. *PLoS One*. 4:e7724.

Tian, M., T. Hagg, N. Denisova, B. Knusel, E. Engvall, and M. Jucker. 1997. Laminin-α2 chain-like antigens in CNS dendritic spines. *Brain Res.* 764:28–38.

Toriyama, M., S. Kozawa, Y. Sakumura, and N. Inagaki. 2013. Conversion of a signal into forces for axon outgrowth through pak1-mediated shootin1 phosphorylation. *Curr. Biol.* 23:529–534.

Toriyama, M., Y. Sakumura, T. Shimada, S. Ishii, and N. Inagaki. 2010. A diffusion-based neurite length-sensing mechanism involved in neuronal symmetry breaking. *Mol. Syst. Biol.* 6:1–16.

Toriyama, M., T. Shimada, K.B. Kim, M. Mitsuba, E. Nomura, K. Katsuta, Y. Sakumura, P. Roepstorff, and N. Inagaki. 2006. Shootin 1: A protein involved in the organization of an asymmetric signal for neuronal polarization. *J. Cell Biol.* 175:147–157.

Won, S., S. Incontro, R.A. Nicoll, and K.W. Roche. 2016. PSD-95 stabilizes NMDA receptors by inducing the degradation of STEP $_{61}$. *Proc. Natl. Acad. Sci.* 113:E4736–E4744.

Zhang, W., and D.L. Benson. 2001. Stages of synapse development defined by dependence on F-actin. *J. Neurosci.* 21:5169–5181.

Zhu, J., Y. Shang, and M. Zhang. 2016a. Mechanistic basis of MAGUK-organized complexes in synaptic development and signalling. *Nat. Rev. Neurosci.* 17:209–223.

Zhu, S., R.A. Stein, C. Yoshioka, C.H. Lee, A. Goehring, H.S. McHaourab, and E. Gouaux. 2016b. Mechanism of NMDA Receptor Inhibition and Activation. *Cell*. 165:704–714.

Ziv, N.E., and S.J. Smith. 1996. Evidence for a role of dendritic filopodia in synaptogenesis and spine formation. *Neuron*. 17:91–102.